Southeastern Geology: Volume 43, No. 2 November 2004

Editor in Chief: S. Duncan Heron, Jr.

Abstract

Academic journal published quarterly by the Department of Geology, Duke University.

SOUTHEASTERN GEOLOGY

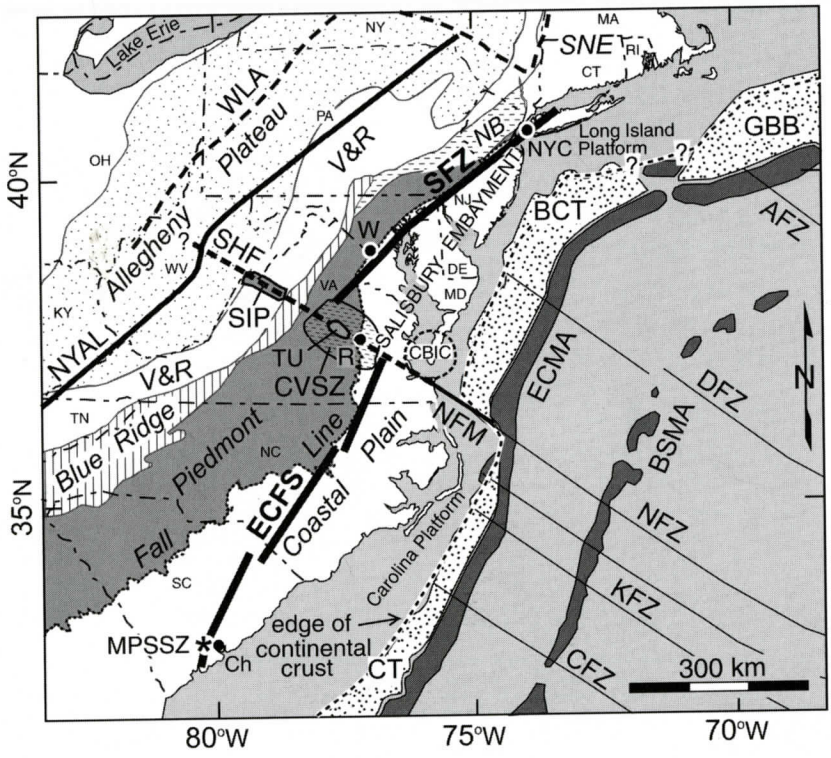

Vol. 43, No. 2 **November 2004**

SOUTHEASTERN GEOLOGY

PUBLISHED

at

DUKE UNIVERSITY

Editor in Chief:

Duncan Heron

This journal publishes the results of original research on all phases of geology, geophysics, geochemistry and environmental geology as related to the Southeast. Send manuscripts to **DUNCAN HERON, DUKE UNIVERSITY, DIVISION OF EARTH & OCEAN SCIENCES, BOX 90233, DURHAM, NORTH CAROLINA 27708-0233**. Phone: 919-684-5321, Fax: 919-684-5833, Email: duncan.heron@duke.edu Please observe the following:

1) Type the manuscript with double space lines and submit in duplicate, or submit as an Acrobat file attached to an email.
2) Cite references and prepare bibliographic lists in accordance with the method found within the pages of this journal. Data citations examples can be found at http://www.geoinfo.org/TFGeosciData.htm
3) Submit line drawings and complex tables reduced to final publication size (no bigger than 8 x 5 3/8 inches).
4) Make certain that all photographs are sharp, clear, and of good contrast.
5) Stratigraphic terminology should abide by the North American Stratigraphic Code (American Association Petroleum Geologists Bulletin, v. 67, p. 841-875).
6) Email Acrobat (pdf) submissions are encouraged.

Subscriptions to *Southeastern Geology* for volume 43 are: individuals - $23.00 (paid by personal check); corporations and libraries - $33.00; foreign $40. Inquires should be sent to: **SOUTHEASTERN GEOLOGY, DUKE UNIVERSITY, DIVISION OF EARTH & OCEAN SCIENCES, BOX 90233, DURHAM, NORTH CAROLINA 27708-0233**. Make checks payable to: *Southeastern Geology.*

Information about SOUTHEASTERN GEOLOGY is on the World Wide Web including a searchable author-title index 1958-2001 (Acrobat format). The URL for the Web site is: http://www.southeasterngeology.org

SOUTHEASTERN GEOLOGY is a peer review journal.

ISSN 0038-3678

SOUTHEASTERN GEOLOGY

Table of Contents

Volume 43, No. 2 November 2004

SOUTHEASTERN GEOLOGY
V. 43, No. 2, November 2004, p.57-80

PROPOSED SHENANDOAH FAULT AND EAST COAST-STAFFORD FAULT SYSTEM AND THEIR IMPLICATIONS FOR EASTERN U.S. TECTONICS

RONALD MARPLE

Houston, TX
ronnmarple@aol.com

PRADEEP TALWANI

Dept. of Geological Sciences,
University of South Carolina, Columbia 29208
talwani@geol.sc.edu

ABSTRACT

Comparison of the Shenandoah igneous province, the central Virginia seismic zone, a northwest-trending linear magnetic anomaly offshore Virginia, and other tectonic features in Virginia suggests the presence of a deep-crustal northwest-trending basement fault, herein named the Shenandoah fault. Along the Shenandoah fault, the central Virginia seismic zone coincides with an apparent ~110 km offset between the northeast-trending Stafford fault zone and East Coast fault system (ECFS).

We postulate that the Stafford fault zone and ECFS formed a continuous ~1100-km-long East Coast-Stafford fault system (EC-SFS) extending from South Carolina to New Jersey before the Alleghanian orogeny. During the Alleghanian or an earlier orogeny, the EC-SFS was beheaded by northwest-vergent thrusting of allochthonous terranes, concealing it beneath those terranes. Late Alleghanian indention in the Salisbury embayment by the Reguibat uplift of northwest Africa produced the Shenandoah fault and offset the EC-SFS left-laterally ~110 km beneath the allochthonous terranes in central Virginia. Late Jurassic to Cenozoic dextral reactivation of the ECFS and Stafford fault at depth fractured the overlying terranes and may have produced north- to northeast-oriented linking faults that reconnected the EC-SFS along a large left-step restraining bend. The cause of the seismicity in central Virginia may be from compression at the bend, which is causing displacements on a variety of faults in the area, including the linking faults, Shenandoah fault, and older Paleozoic faults.

Late Jurassic and middle Eocene dextral deformation along the large restraining bend along the EC-SFS in central Virginia produced tension across the Shenandoah fault to the northwest. This tension caused normal-sense reactivation of the fault beneath the allochthonous terranes of the Blue Ridge and Valley and Ridge provinces. Consequently, magma migrated up the Shenandoah fault and then along bedding planes and northwest joints within the Valley and Ridge strata to form the Shenandoah igneous province.

INTRODUCTION

Although great advances have been made in recent decades toward understanding the tectonic development of the eastern U.S., certain aspects have remained controversial. The nature of the Alleghanian indention in the Salisbury embayment area and whether it even occurred is a good example. Several studies have argued for different styles of indention by the Reguibat uplift of northwest Africa (e.g., Lefort, 1988) while other studies have argued against the indention (e.g., Sheridan and others, 1999). Other examples of features in the eastern U.S. whose origins have remained largely enigmatic include the central Virginia seismic zone, Stafford fault zone, and Shenandoah igneous province in western Virginia (Figure 1).

The purpose of this study was to investigate

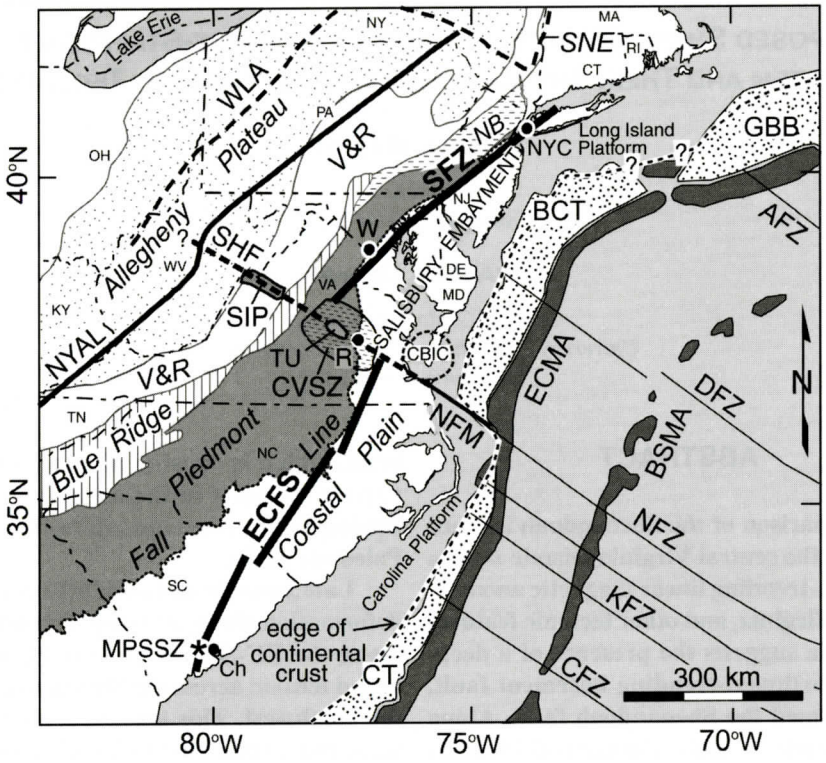

Figure 1. Locations of the proposed East Coast-Stafford fault system (defined by the ECFS and Stafford fault zone (SFZ), NNE-trending solid lines), Shenandoah basement fault (SHF, dashed line onshore and solid line offshore), Shenandoah igneous province (SIP, contoured area), central Virginia seismic zone (CVSZ, stippled area), western limit of Alleghanian deformation (WLA, dashed line, modified from Hatcher and others, 1989, and Wintsch and others, 1992), linear magnetic anomaly offshore Virginia (NFM, solid line, Behrendt and Grim, 1985), New York-Alabama lineament (NYAL, solid line, King and Zietz, 1978), Chesapeake Bay impact crater (CBIC), topographic uplift (TU) of Krohn and Phillips (1982), and the Middleton Place-Summerville seismic zone (MPSSZ, star). Dashed line near west edge of offshore sedimentary troughs denotes approximate edge of continental crust (e.g., Glover and others, 1997). Physiographic provinces are generalized from Hack (1989). Oceanic fracture zones, south to north, are from Klitgord and Schouten (1986): CFZ, Carolinas; KFZ, Kane; NFZ, Norfolk; DFZ, Delaware Bay; AFZ, Atlantis. BSMA, Blake Spur magnetic anomaly; ECMA, East Coast magnetic anomaly; NB, Newark rift basin (short dashed pattern); SNE, southern New England physiographic provinces; V&R, Valley and Ridge province. Offshore Triassic rift basins: CT, Carolinas Trough; BCT, Baltimore Canyon Trough; GBB, Georges Bank Basin. Cities from southwest to northeast: Ch, Charleston, South Carolina; R, Richmond, Virginia; W, Washington, DC; NYC, New York City.

the cause of these and other features in the eastern U.S. using a variety of geologic, geophysical, and seismicity data. Our results suggest that late Alleghanian (Late Permian) indention created the northwest-trending Shenandoah fault and offset the EC-SFS beneath the Blue Ridge-Piedmont megathrust sheet complex. They also suggest that the central Virginia seismic zone and Shenandoah igneous province are associated with displacements on the proposed East Coast-Stafford fault system (EC-SFS) and Shenandoah fault. The general development of these fault systems and associated features are summarized in Figure 2.

ECFS AND STAFFORD FAULT ZONE

The proposed EC-SFS consists of two major

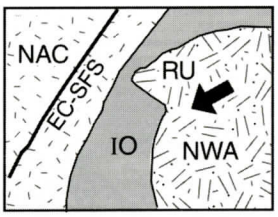

A. Continuous EC-SFS before late Alleghanian headon indention.

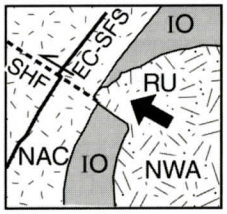

B. Initial formation of SHF by initiation of headon indention (Early Permian).

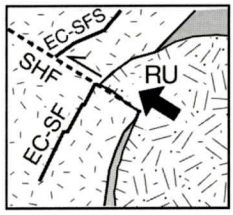

C. Continued indention by Reguibat uplift during Early Permian time.

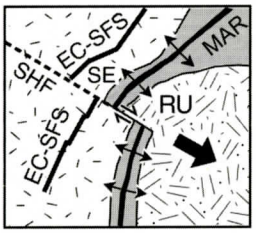

D. Onset of early Mesozoic rifting.

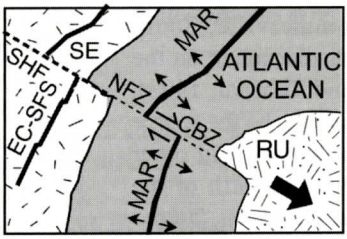

E. Continued rifting since the early Mesozoic with development of Norfolk and Cape Blanc fracture zones.

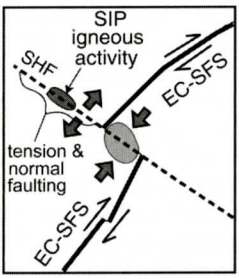

F. Late Jurassic and mid-Eocene intrusive igneous activity in Shenandoah igneous province.

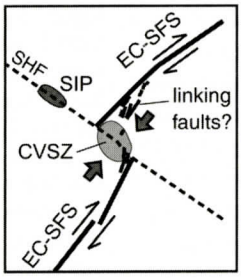

G. Cenozoic development of seismicity and linking faults at the EC-SFS offset.

Figure 2. General evolution of the EC-SFS, Shenandoah fault (SHF, dashed line), central Virginia seismic zone (CVSZ), and Shenandoah igneous province (SIP). For simplicity, diagrams do not include Alleghanian allochthonous terranes or the rotation of Africa presented by Hatcher (2002). Diagrams A-C illustrate how late Alleghanian head-on indention created the SHF and offset the EC-SFS (relative motion of Africa in diagram A is modified from Hatcher, 2002). Diagrams D and E demonstrate how the SHF later became aligned with the Norfolk fracture zone (NFZ) as the mid-Atlantic ridge (MAR) developed after early Mesozoic rifting (shaded area is early Atlantic Ocean). Diagram F shows how impingement of the crust east of the EC-SFS on the crust to the west during dextral movement caused tension, normal faulting, and igneous activity (SIP) along the SHF to the northwest beneath the allochthonous terranes. Diagram G illustrates how late Mesozoic and Cenozoic dextral movement on the EC-SFS has produced compression, seismicity, and possibly linking faults across the EC-SFS offset. Dark arrows in A-E denote movement of northwest Africa relative to North America. CBZ, Cape Blanc fracture zone; IO, Iapetan Ocean (shaded area in diagrams A-C); NAC, North American craton; NWA, northwest African craton; RU, Reguibat uplift; SE, Salisbury embayment.

segments: the East Coast fault system (ECFS) and Stafford fault zone. The ECFS dips >80° to the northwest in South Carolina and consists of three ~200 km long segments offset ~15 km in a right-step sense from each other (Marple and Talwani, 2000) (Figure 1). These segments are mostly buried beneath Coastal Plain sediments and are defined by local anomalous changes in river morphology that coincide with evidence of buried faulting and folding of sediments. Seismic focal mechanisms along the southern end of the ECFS near Summerville, South Carolina, indicate dextral displacement on the ECFS (e.g., Madabhushi and Talwani, 1993). The ECFS in South Carolina may be the source of the 1886 Charleston earthquake and other Holocene earthquakes near and north of the Summerville area (Marple and Talwani, 2000).

From central Virginia northward, the Stafford fault zone is also buried beneath the Coastal Plain sediments and is defined by drill-hole, river morphology, and seismicity data (e.g., Marple, 2004). The Stafford fault zone dips steeply to the northwest and displays west-side-up offsets that decrease upward through the Coastal Plain sediments (Mixon and others, 1992). Trench studies across a segment of the Stafford fault in north-central Virginia indicate a component of dextral displacement (e.g., Mixon and Newell, 1977).

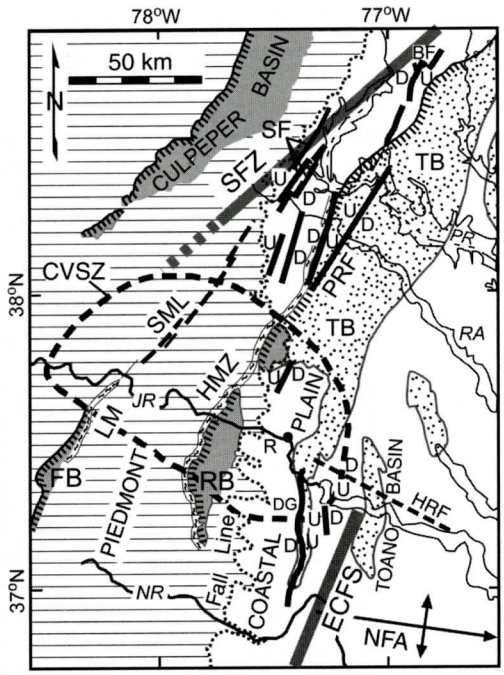

Figure 3. Map of central Virginia comparing the ECFS, Stafford fault zone (SFZ), Cenozoic faults along the inner Coastal Plain (thick black lines, U on upthrown side), Paleozoic faults (labeled), and buried (dotted pattern) and exposed (shaded) early Mesozoic rift basins. Hachures along west side of basins denote southeast dip of border faults. Faults and basins are taken from Mixon and others (1989, 1992), Benson (1992), Geologic Map of Virginia (1993), and Wilkes (1993). Most Cenozoic faults between the ECFS and SFZ dip steeply to the northwest whereas the basin border faults dip southeastward and become listric at depth. CVSZ, central Virginia seismic zone (dashed contour); FB, Farmville basin; HMZ, Hylas mylonite zone; LM, Lakeside mylonite zone; NFA, Norfolk arch; RB, Richmond basin; SML, Spotsylvania magnetic lineament; TB, Taylorsville basin. Faults: BF, Brandywine; DG, Dutch Gap; HRF, Hampton Roads (dashed); PRF, Port Royal; SF, Stafford fault system of Mixon and others (1992). Rivers from south to north: NR, Nottoway; JR, James; RA, Rappahannock; PR, Potomac.

Crosscutting Nature of the ECFS and Stafford Fault

Another characteristic of the ECFS and Stafford fault is that they crosscut Paleozoic and early Mesozoic terranes and structures. This crosscutting relationship suggests that they formed since the end of early Mesozoic rifting or that they are reactivated pre-Alleghanian basement faults that fractured through the overlying terranes. The ECFS, for example, crosscuts the Paleozoic southeast-dipping faults of the Eastern Piedmont fault system of Hatcher and others (1977), as well as Triassic basins in South Carolina (see Figure 1 of Marple and Talwani, 2000). Beneath the South Carolina Coastal Plain, the seismically defined Woodstock fault (southern end of the ECFS) dips >80° to the northwest at ~7 to 13 km depths (Madabhushi and Talwani, 1993). In contrast, the Paleozoic faults located east and west of the buried Woodstock fault dip southeastward.

Table 1. Acquisition Parameters for Amoco Seismic-Reflection Profile near Augusta, Virginia*

Source type	4 Vibroseis vibrators (model Y-600RD)
Source array	15 m spacing inline
Source duration	7 sec
Source interval	330 ft (~100 m)
Sweep frequency range	14 – 56 Hz, spike
Geophone group spacing	330 ft (~100 m)
Geophone array	24 phones inline with 10 Hz natural frequency, 4 m spacing
Filters	12 – 62.5 Hz
Line array	48 channels, split spread
Typical spread dimensions	2710-400-400-2710 (distances in m)
Recording time	12 sec
Sample rate	4 ms
Subweathering velocity	3650 m/s

*Data provided courtesy of Seismic Exchange, Inc., Houston, Texas.

Similarly, the Stafford fault segment in northern Virginia dips steeply to the northwest, whereas the shear zones associated with the Paleozoic-age Lakeside and Hylas mylonites, as well as other Paleozoic and early Mesozoic faults to the east and west, generally dip southeastward (e.g., Figure 10 of Marple, 2004) (Figure 3). To the northeast, the steep northwest-dipping fault plane solution and aftershock distribution of the 1973 Wilmington, Delaware, earthquake (Sbar and others, 1975) indicate that the Stafford fault zone crosscuts the southeast-dipping Paleozoic thrust faults near the Delaware River bend (Marple, 2004).

DATA AND METHODS

To determine their relationships and origins, we compared the ECFS, Stafford fault zone, central Virginia seismic zone, and Shenandoah igneous province with other tectonic features along the U.S. Atlantic margin. To accomplish this, we integrated geologic, geophysical, and seismicity data from a variety of sources.

We also reprocessed a set of commercial digital seismic-reflection data from western Virginia using Disco version 12.1 software to search for faulting in the Shenandoah igneous province (Table 1). Because igneous rocks, such as basalt, typically produce higher seismic velocities than most sedimentary rocks (Touloukian and others, 1981), such as those in the Valley and Ridge, we used velocity analyses of the pre-stack seismic-reflection data to infer the presence of igneous sills and dikes. Valley and Ridge strata comprise the upper 2 to 2.2 sec (two-way traveltime [TWTT]) and generally consist of dolostone, limestone, shale, and sandstone rocks (Harris and Milici, 1977) (Figure 4B). Reflection events in the underlying basement are more discontinuous and dip mostly to the northeast. The upper 700 ms of data are not shown because of their poor data quality. Unfortunately, no deep drill-hole data existed nearby to determine the age or rock type of reflection events.

EVIDENCE FOR A NORTHWEST-TRENDING BASEMENT FAULT

One set of evidence for a northwest-trending (~N60°W) basement fault in Virginia is inferred from northwest-trending fault plane solutions from the central Virginia seismic zone at the offset between the ECFS and Stafford fault zone. This cluster of seismicity, measuring ~120 km north-south by ~150 km east-west (Figures 1, 3, and 5), is characterized by a mixture of steep (>60°) northeast-trending strike-slip and northwest-trending reverse fault-plane solutions at about 3 to 13 km depths (Bollinger and others, 1991).

Other evidence for the northwest-trending fault is inferred from the northwest elongate, 60 km by 30 km area of northwest-trending, Late Jurassic (~157-144 Ma) alkalic dikes and middle Eocene (~48-35 Ma) alkalic to mafic dikes, plugs, sills, and diatremes in the Valley and Ridge province of western Virginia known as the Shenandoah igneous province (e.g., Tso and others, 2004) (SIP, Figures 1 and 4A). Most investigators of the SIP have concluded that it is associated with a deep-crustal, northwest-oriented basement fault beneath the imbricate thrust complex of the Valley and Ridge Province (e.g., Southworth and others, 1993). The diatremes, minor contact metamorphism, initial Sr^{87}/Sr^{86} ratio of 0.704 for the felsic intrusives (Fullagar and Bottino, 1969), and low levels of the large-ion-lithophile elements K, Rb, and Cs in the Eocene felsic intrusive rocks (Southworth and others, 1993) indicate that the felsic magmas rapidly ascended from the upper mantle or lower crust with little or no crustal contamination, probably along a deep-crustal fault.

Seismic-Reflection Evidence for a Basement Fault in the Shenandoah Igneous Province

The ~26-km-long seismic-reflection profile that we reprocessed supports the existence of a northwest-trending basement fault in the Shenandoah igneous province. Near the center of Figure 4B, the lower part of the Valley and Ridge strata between 1.7 and 2.2 sec is offset down to the northeast along a steep, northeast dipping fault plane, indicating normal-sense displacement. The offset decreases upward from ~100 ms TWTT (~300 m) at the basement interface (just below event C) to ~60 ms TWTT (~170 m) along the strong reflector at ~1.75 sec (event B), indicating recurrent normal movement since the Paleozoic era. This post-Paleozoic reactivation is inferred from the fault's vertical continuity across the basement/allochthon boundary. Otherwise, the fault segments above and below the boundary would have become unaligned during the westward transport

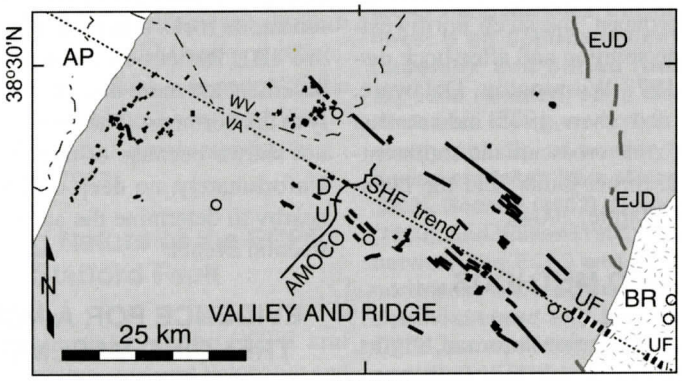

A.

Figure 4. A. Map of Shenandoah igneous province (black solid lines and patterns) with the approximate locations of Shenandoah fault (SHF, thin dotted line) and Amoco seismic-reflection profile (with normal fault, D on downthrown side) shown. Gray lines labeled EJD are Early Jurassic diabase dikes and UF denotes faults of unknown type (dashed lines). Open circles are small (magnitude > 1.0) earthquakes recorded between 1974 and 1988 (Çoruh and others, 1988). AP, Allegheny Plateau province; BR, Blue Ridge province. Modified from Southworth and others (1993) and Rader and Wilkes (2001). B. Portion of time migrated seismic-reflection profile acquired by Amoco in 1982. Dashed lines denote reflection events A, B, and C. TB denotes top of basement. Note the fault offsetting deeper Valley and Ridge strata between about 1.3 and 2.2 sec two-way travel time (TWTT). Seismic data provided by Seismic Exchange, Inc., Houston, Texas, and reprocessed by the first author with permission from Geosignal, Inc., Division of WesternGeco, Houston, Texas.

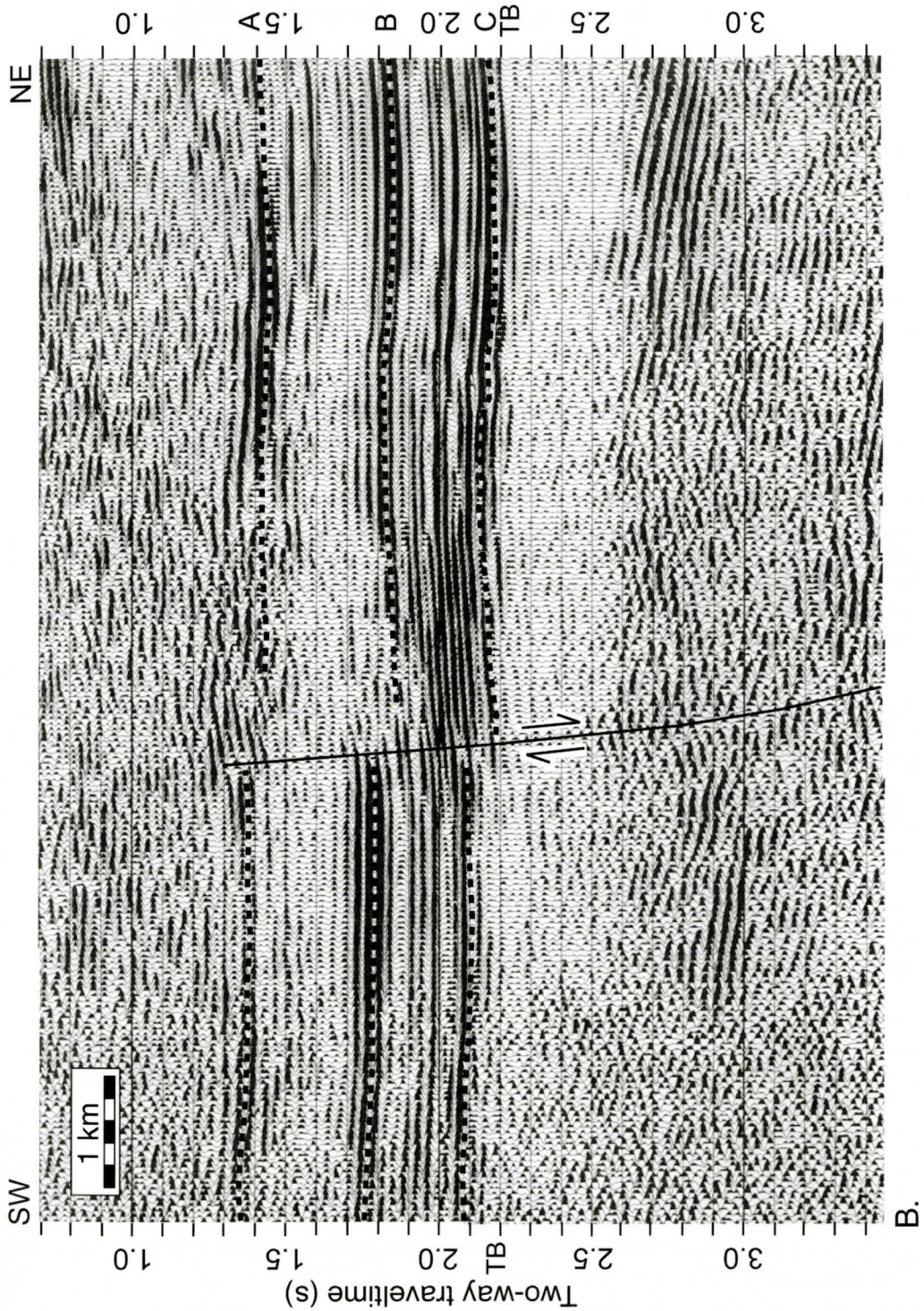
NE
SW
A
B
C
TB
TB
1 km
1.0
1.5
2.0
2.5
3.0
Two-way traveltime (s)
B.

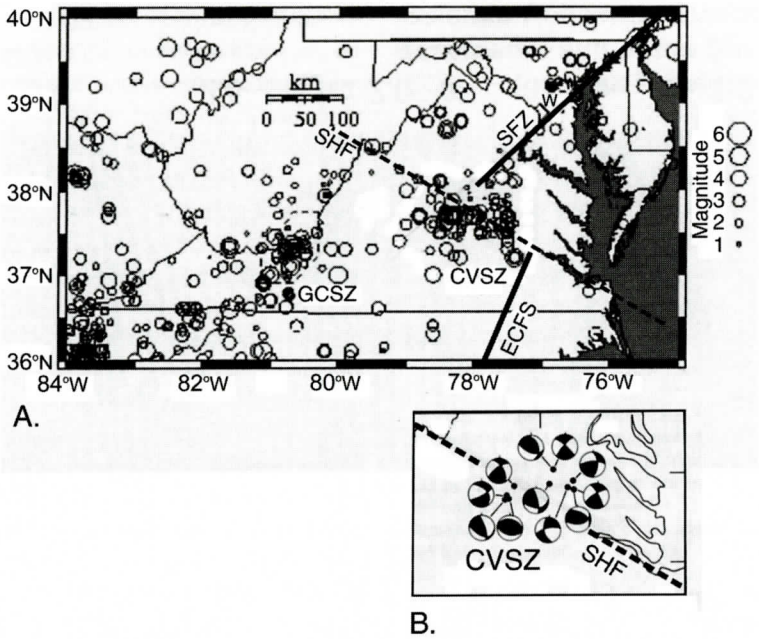

Figure 5. A. Seismicity in and near Virginia from 1774-1994 compared to ECFS and Stafford fault zone (SFZ). Note the location of the central Virginia seismic zone (CVSZ) between the ECFS and SFZ. GCSZ, Giles County seismic zone; SHF, Shenandoah fault; W, Washington, DC. B. A few focal mechanism solutions (orthogonal nodal planes with compressional quadrants shaded) of small earthquakes in the CVSZ. Modified from Bollinger and others (1991).

of the Valley and Ridge thrust sheet complex during the Alleghanian orogeny. Post Paleozoic normal movement is also inferred from the Middle Jurassic and Eocene igneous activity in the province, which occurred contemporaneously with the normal-sense reactivation of the fault.

Several igneous sills just above reflection event C near the fault are inferred from high amplitudes, higher velocities interpreted from velocity analyses (~1.2 km/s faster for reflections between events B and C on the downthrown (northeast) side of the fault), and the greater number of events northeast of the fault. Near the northeast side of the fault at ~1.4 sec TWTT are several strong southwest-dipping discontinuous crosscutting events that have higher amplitudes and velocities. These characterics suggest that the crosscutting events are dikes extending away from the fault. Magma migrated up the fault and then along bedding planes and preexisting northwest-trending joints, like those that are common throughout the central Appalachians (e.g., Zhao and Jacobi, 1997). Vertical dikes are not evident on the seismic profile because the resolution of these data is unsuitable to image them (see also Badley, 1985). The offset of reflector C and the chaotic appearance and opposing dips beneath the Valley and Ridge strata suggest that the fault offsets the basement rocks. The fault's location in the middle of the Shenandoah igneous province suggests that it was a conduit for the igneous activity in the Shenandoah province. Hence, it is named the Shenandoah fault.

Other Evidence for a Northwest-Trending Basement Fault

Other evidence for a northwest-trending basement fault includes: (1) an ~150-km-long, northwest-trending linear magnetic anomaly (NFM in Figure 1) in continental crust, which is associated with a strike-slip shear zone northwest of the Norfolk fracture zone (Behrendt and Grim, 1985); (2) basement faulting on marine

seismic-reflection profile 12 of Klitgord and others (1994) at NFM; (3) an ~110 km left-lateral offset of the continental margin offshore that coincides with part of NFM; (4) an ~30 km offset of the Precambrian basement fault associated with the ~1600-km-long New York–Alabama lineament (NYAL) (King and Zietz, 1978); and (5) a 40- by 20-km-long topographic uplift west of Richmond, Virginia, inferred from Landsat satellite data and field reconnaissance (Krohn and Phillips, 1982) (Figure 1).

Cederstrom (1945) interpreted a buried fault along this trend in the Virginia Coastal Plain that they called the Hampton Roads fault (Figure 3). Powars and Bruce (1999), though, noted that the southeastern end of this fault is associated with the southern rim of the Eocene-age Chesapeake Bay impact crater (Figure 1). More detailed data are needed to determine if the northwest segment of this fault is associated with the impact crater or with the proposed Shenandoah fault.

DISCUSSION

Correlation of the ECFS and Stafford Fault

Although the ECFS and Stafford fault zone are buried beneath the Coastal Plain sediments, indirect evidence supports their correlation across the central Virginia offset. First, both of these fault systems dip steeply to the northwest, both are linear, both share a common post-early Mesozoic history as indicated by their crosscutting nature, and both show evidence for Cenozoic dextral displacement (e.g., Madabhushi and Talwani, 1993; Marple, 2004). The crosscutting characteristic of these two fault systems is unique because nowhere else along the U.S. Atlantic margin are there long faults like these that crosscut the Paleozoic terranes and Triassic basins. Secondly, the mixture of northwest- to northeast-trending fault plane solutions of small earthquakes between the two fault systems (Bollinger and others, 1991) is consistent with seismicity patterns at fault offsets (Talwani, 1999; Gangopadhyay and Talwani, 2003). We, therefore, propose that the ECFS and Stafford fault were once a continuous East Coast-Stafford fault system (EC-SFS) that was offset during late Alleghanian indention.

Origin of the East Coast-Stafford Fault System (EC-SFS)

The fact that the EC-SFS crosscuts the Paleozoic and Triassic terranes and structures (Figure 1 of Marple and Talwani, 2000; Figure 10 of Marple, 2004) indicates that either it formed since the end of early Mesozoic rifting or it is a reactivated pre-Alleghanian basement fault system that has fractured the overlying terranes (Figures 6 and 7). It is unlikely, though, that a late Mesozoic or Cenozoic regional compressive stress field could have produced such a new, long crosscutting fault system through the allochthonous terranes because the similarly-oriented, northeast-trending Paleozoic thrust faults and shear zones throughout the Coastal Plain and Piedmont provinces could have accommodated the regional strain. This hypothesis is supported by the repeated reactivation of the Paleozoic faults during the Alleghanian orogeny and again during early Mesozoic rifting. Moreover, there is evidence for Cenozoic reactivation of some Paleozoic and early Mesozoic faults from seismicity and trenching studies (e.g., Bramlett and others, 1982). Thus, a more likely cause of the crosscutting relationship is that late Mesozoic or Cenozoic reactivation of a pre-Alleghanian basement fault system fractured through the overlying terranes (Figure 7). This basement origin is analogous to the Precambrian basement fault to the west associated with the New York-Alabama lineament (NYAL) (e.g., Johnston and others, 1985) (Figure 1), except for the fracturing of the overlying allochthonous terranes by the ECFS and Stafford fault (e.g., Marple, 2004). Unfortunately, unlike the sedimentary rocks of the Allegheny Plateau along the NYAL, the higher magnetization and greater thickness (7 to 15 km) of the Blue Ridge and Piedmont allochthonous terranes to the east makes detection of the pre-Alleghanian ductile roots of the EC-SFS difficult using potential field data.

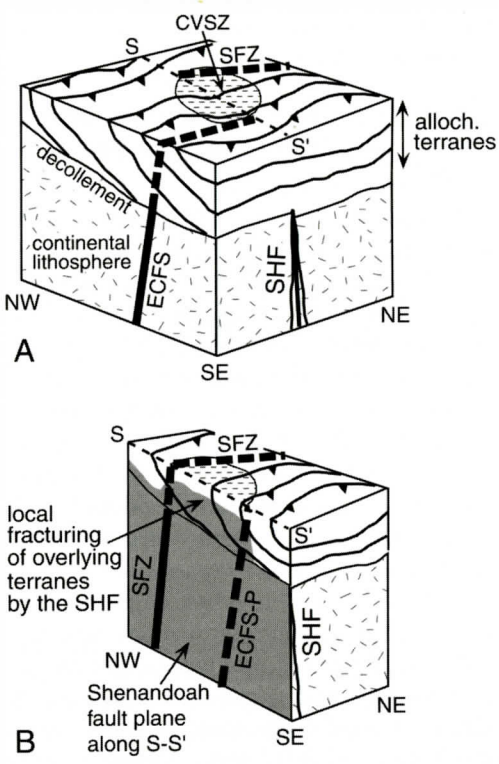

Figure 6. Conceptual models (not to scale) illustrating the basement origin of the ECFS, Shenandoah fault (SHF), Stafford fault zone (SFZ) (Coastal Plain sediments removed and linking faults not shown). Vertical exaggeration is about 7X. The ECFS and Stafford fault are dashed in the overlying allochthonous terranes. Dashed line S-S' represents the surface projection of the Shenandoah fault. Pattern of short dashes at the surface denotes central Virginia seismic zone (CVSZ). Diagram B is the northeast half of diagram A with the Shenandoah fault plane exposed (gray pattern). ECFS-P (dashed line) denotes the northeastward projection of the ECFS onto the Shenandoah fault plane. Fracturing of the overlying allochthonous terranes along the Shenandoah fault (gray pattern above décollement) between the ECFS and Stafford fault zone is inferred from the northwest-oriented fault plane solutions of the central Virginia seismic zone.

We also considered the possibility that the ECFS and Stafford fault were produced by early Mesozoic rifting with the Shenandoah fault as a transfer fault between the two segments (Figure 8A). This hypothesis is unlikely, though, for at least two reasons. First, there is no evidence for normal displacement on the ECFS or Stafford fault. Available evidence indicates dextral and up-to-the-northwest reverse displacement (e.g., Marple, 2004). Secondly, the Paleozoic terrane boundaries at the surface are not laterally displaced along the Shenandoah fault trend between the Stafford fault and the coast. We, therefore, favor the hypothesis that the EC-SFS is a pre-Alleghanian basement fault system and that its post-early Mesozoic reactivation fractured the overlying allochthonous terranes.

Origin of the Shenandoah Fault

The northwest trend of the Shenandoah fault across the northeast-trending Paleozoic terranes and Triassic basins, the lack of surface faulting along its trend, and the normal fault on the Amoco seismic-reflection profile suggest that the Shenandoah fault is a basement fault beneath the allochthonous terranes (Figures 4B and 6). Its collinear alignment with the Norfolk fracture zone and offset in the continental margin (Figure 1) suggests either a late Alleghanian or early Mesozoic origin. Previous studies proposed that the Norfolk fracture zone continued northwestward through North American crust (e.g., Fletcher and others, 1978). However, as Sykes (1978, p. 625) explained, Mesozoic oceanic fracture zones cannot exist in pre-Mesozoic continental crust. A more likely explanation for the alignment of the Shenandoah fault and Norfolk fracture zone is inferred from their coincidence with the offset in the continental margin. This offset, combined with the late Paleozoic juxtaposition of the Salisbury embayment and Reguibat uplift of northwest Africa (e.g., Klitgord and Schouten, 1986) (Figure 9), strongly suggests that the Shenandoah fault formed either during Triassic rifting or during late Alleghanian indention by the Reguibat uplift. The rifting scenario is unlikely, though, because the extensional forces required to produce a 600-km-long, northwest-trending strike-slip fault with tens of kilometers displacement would have produced more normal faulting in the southeastern U.S. than in the mid-Atlantic states and should have left-laterally offset the

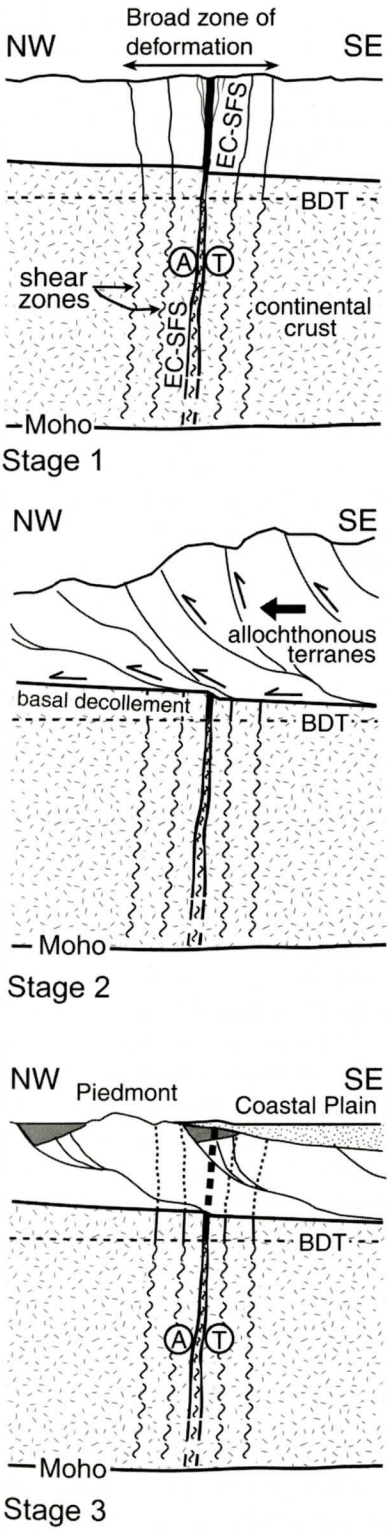

overlying allochthonous terranes, neither of which is true (Figure 8B).

Based on these arguments and the deep-crustal or mantle origin of the Shenandoah Eocene igneous intrusive rocks, it is more likely that the Shenandoah fault is a deep-crustal fault zone produced by head-on (northwest) indention during late Alleghanian (Early Permian) collision (Figures 2B-2C). This hypothesis is supported by the late Paleozoic fit of the continents and northwest curvature of aeromagnetic and structural patterns around the Salisbury embayment (e.g., Lefort and Max, 1991). Note especially the alignment of the Shenandoah fault with the Cape Blanc fault (CBF) along the southwest edge of the Reguibat uplift (Figure 9). Indention also can explain the large decrease in displacement northwestward along the Shenandoah fault (Figure 1). The resulting offset margin then could have produced an offset in the initial rift zone during early Mesozoic rifting, thus resulting in the Norfolk fracture zone (Figures 2D-2E). Thus, it is likely that late Alleghanian indention produced the Shenandoah fault.

Offsets Produced by Alleghanian Indention

Several investigators have concluded that northwest Africa indented the Salisbury embayment area during the Alleghanian orogeny (e.g.,

Figure 7. Conceptual model illustrating how the EC-SFS between South Carolina and Long Island was beheaded by westward transport of the Blue Ridge-Piedmont megathrust sheet complex during the Alleghanian orogeny. Stages in the evolution of the EC-SFS: 1) Formation of the EC-SFS as a strike-slip fault system during the Acadian or earlier orogeny. Fault displacement mainly was oblique, up-to-the-west dextral (A, away from observer; T, toward observer). BDT is brittle-ductile transition zone. 2) The fault system in the upper crust was beheaded by westward movement of the allochthonous terranes over the craton during the Alleghanian orogeny. 3) Reactivation of the EC-SFS beneath the allochthonous terranes by late Jurassic to Cenozoic dextral transpression produced new brittle faulting (dashed lines) through the overlying terranes.

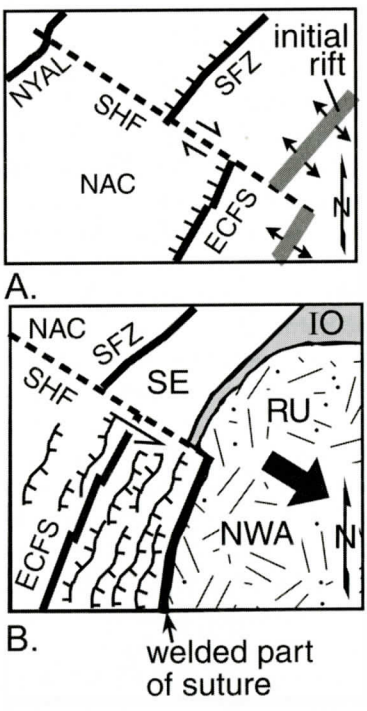

Figure 8. Other mechanisms considered to determine the origin of the Shenandoah fault (SHF), ECFS, and Stafford fault zone (SFZ). Diagram A shows the ECFS and Stafford fault as early Mesozoic normal faults with down-to-the-northwest displacement (tick marks on downthrown side). NAC, North American craton; NYAL, New York-Alabama lineament. Diagram B shows the southeastern U.S. and Africa welded together (thick black line) at the end of the Alleghanian orogeny. Tick marks denote the downthrown side. IO, Iapetan Ocean (shaded area); NWA, northwest African craton; RU, Reguibat uplift; SE, Salisbury embayment.

Lefort and Max, 1991).

Their conclusions generally were based on the northwest curvature of aeromagnetic and structural patterns around the Salisbury embayment (e.g., Lefort, 1988), the late Paleozoic fit of North America and northwest Africa (e.g., Klitgord and Schouten, 1986), the presence of easterly derived late Mississippian through Early Permian clastic sediment in the central Appalachians of Pennsylvania and New York (Hatcher, 2002), and the Alleghanian strike-slip fault motions in the southeastern U.S. and in the Mauritanian orogenic belt southwest of the Reguibat uplift, which are consistent with the southward escape of the terranes (Vauchez and others, 1987). According to Lefort and Max's (1991) model, an extension of the Reguibat uplift indented the area during the later part of the Alleghanian orogeny; the Reguibat uplift is a Precambrian shield in the West African craton that may be as much as 70 km thick (Toft and others, 1992). They concluded that either part of the Reguibat uplift remained beneath the Coastal Plain during early Mesozoic rifting or the Paleozoic terranes were crushed together in the Salisbury embayment area during indention. Their model assumes that the indention was symmetric, but this would have produced dextral strike-slip faulting south of the embayment and sinistral faulting to the north (Hatcher, 1989). Because faults both north and south of the embayment underwent mainly dextral deformation during the early Alleghanian, Hatcher (2002) concluded that northwest Africa collided obliquely and rotationally from northeast to southwest. He did not continue the indention during late Alleghanian (Early Permian) head-on collision because of the lack of sinistral strike-slip faulting in southern New England. However, the northwest transport of the Blue Ridge-Piedmont megathrust sheet complex over the continental margin by the relative northwestward movement of Africa during the late Alleghanian (e.g., Figure 1 of Hatcher, 2002) required that the Reguibat uplift continue indenting the continental margin, though head-on rather than oblique like the early Alleghanian indention. Thus, the lack of sinistral strike-slip faulting in southern New England alone cannot be used to argue against head-on indention. The lack of sinistral faulting in southern New England may be explained in at least two ways. Perhaps most of the compressional deformation of the allochthonous terranes was concentrated too far eastward in the Salisbury embayment and continental shelf (cross-section B-B' of Figure 10) to cause lateral escape in southern New England. Alternatively, much of the lateral escape of the allochthonous terranes occurred before Late Alleghanian head-on indention.

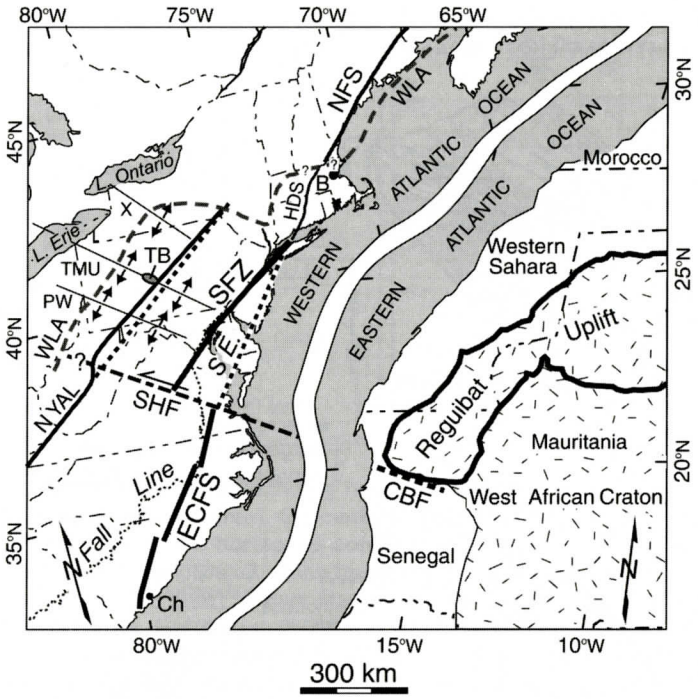

Figure 9. Juxtaposition of Reguibat uplift (bold outline within West African craton, patterned area, Weigel and others, 1982; Deynoux and others, 1982; Lécorché and others, 1983) and Salisbury embayment (SE). The northeast projections of the ECFS and southern NYAL are denoted by dashed lines. Opposing arrows on the northwest-trending lineaments denote Alleghanian, northeast-oriented extension northwest of the Salisbury embayment. TB denotes area of normal faulting (Tipton block, Faill, 1981) along TMU. Northwest-trending lineaments: PW, Pittsburgh-Washington; TMU, Tyrone-Mt. Union; and unnamed lineament X (Lavin and others, 1982). CBF, Cape Blanc fault (dashed line, Lefort and Max, 1991; Lécorché and others, 1983); HDS, Higganum dike system; NFS, Norumbega fault system; WLA, western limit of Alleghanian deformation (dashed contour); SFZ, Stafford fault zone; SHF, Shenandoah fault (dashed line). Cities: B, Boston, Massachusetts; Ch, Charleston, South Carolina.

Our results suggest that the indention continued during the late Alleghanian (Early Permian) head-on collision, but without a large fragment of African crust beneath the embayment. Head-on (northwest) indention is supported by the linear ~N60°W-orientation of the Shenandoah fault and its near parallelism with the late Alleghanian thrust transport vectors of Hatcher (2002). In contrast to Lefort and Max's (1991) hypothesis, we postulate that the Reguibat uplift was oriented obliquely relative to the embayment during head-on (northwest) indention so that it produced a wedge-shaped indentation and the deep-crustal Shenandoah fault to the south beneath the allochthonous terranes (Figures 2B-2C and 10). The wedge-shaped indentation is further supported by the more northeasterly trends of the New York–Alabama lineament (NYAL) and Stafford fault zone north of the Shenandoah fault than the NYAL and ECFS trends to the south (Figure 9). Because there is no evidence for large fragments of African craton beneath the embayment (Sheridan and others, 1999), the edge of the Reguibat indentor likely did not extend farther west than the present outer continental shelf. In the craton beneath the allochthonous terranes, the indention offset the originally continuous EC-SFS and the NYAL ~110 and ~30 km, respectively, along the Shenandoah fault (Figures 1 and 10). This large decrease in offset northwestward along the Shenandoah fault indicates

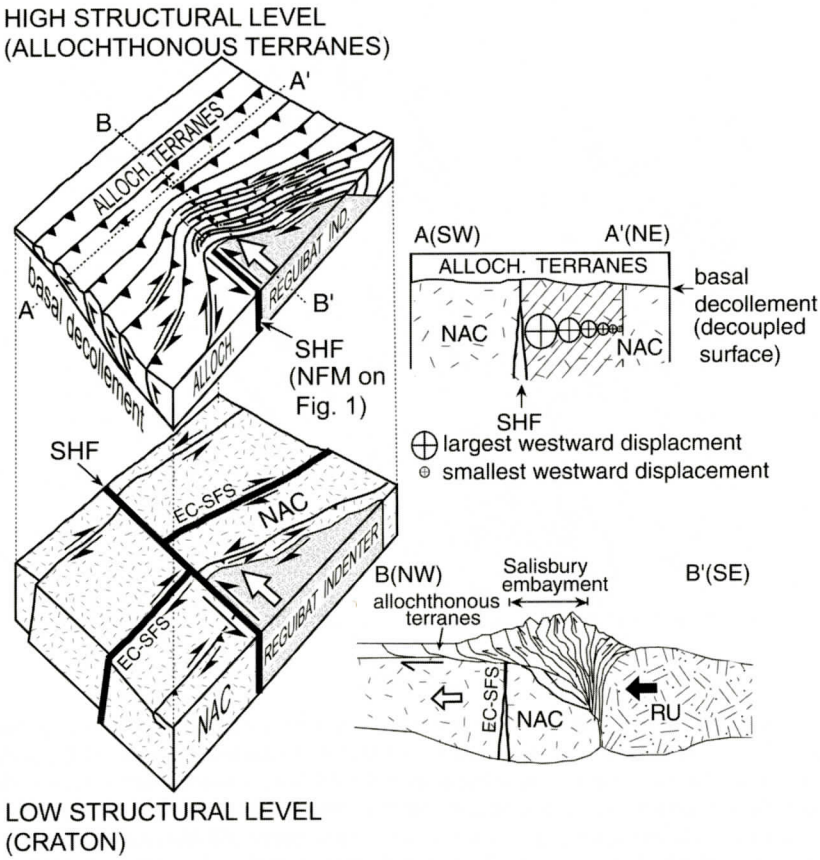

Figure 10. Conceptual model illustrating indention of Salisbury embayment area by Reguibat uplift during late Alleghanian head-on collision. Upper left diagram consists of the Blue Ridge-Piedmont allochthon and Valley and Ridge fold-thrust belt, and lower left diagram is underlying North American craton. The craton northeast of the newly created Shenandoah fault (SHF) was pushed northwestward beneath the allochthonous terranes by the Reguibat indentor (striped area, cross section AA' in lower right; see also cross section BB'). The dark arrow in cross section BB' indicates the northwest collision of the Reguibat uplift (RU) with the North American craton (NAC) while the open arrow indicates the northwestward movement of the North American craton (northeast of Shenandoah fault) beneath the allochthon in response to the Reguibat indentor.

that compressional deformation was concentrated in the zone of impact near the margin (Figure 10). The crustal shortening beneath the allochthon north of the Shenandoah fault could have been accommodated by a variety of indentor-related processes, such as northeastward lateral escape between basement faults like the Stafford fault and NYAL, by assimilation of the lower part of the thickened crust north of the Shenandoah fault by the upper mantle, or perhaps by subduction of North American continental crust beneath the allochthon into the mantle north of the Shenandoah fault (e.g., Tapponnier and others, 2001).

In contrast, the indention did not laterally offset the allochthonous terranes along the Shenandoah basement fault, except perhaps near the continental margin where they are now buried by thick sediments (Figure 1). This observation can be explained in at least two ways. In contrast to the more coherent craton, the many preexisting thrust faults of the overlying terranes near the zone of indention accommodated most of the indenter-related compression-

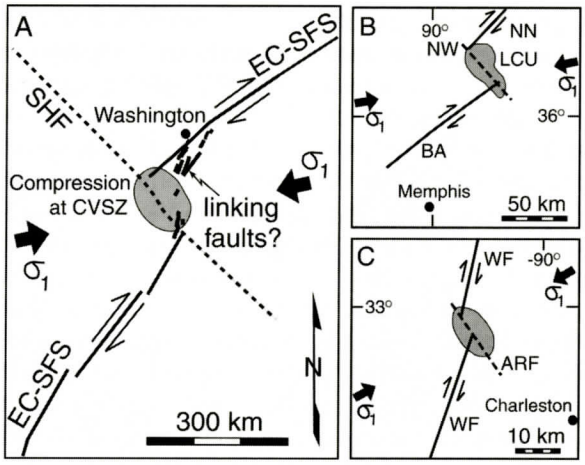

Figure 11. A. Conceptual model demonstrating how dextral motion on the EC-SFS has produced compression at the bend (shaded area), the central Virginia seismic zone (CVSZ), and possibly linking faults. Regional maximum horizontal compressive stress, σ_1, denoted by solid arrows (Zoback and Zoback, 1991). SHF, Shenandoah fault (dashed line). B. Map illustrating geometry of faults and seismicity (shaded area) in New Madrid seismic zone where BA, NW, NN, and LCU denote the Blytheville Arch, Northwest and North New Madrid faults, and Lake County Uplift, respectively. C. Map of seismicity (shaded area) and faults near Summerville, South Carolina. ARF, Ashley River fault; WF, Woodstock fault; Note the concentration of seismicity on both maps B and C at fault offsets. Diagrams B and C are modified from Talwani (1999).

al deformation of the terranes in the Salisbury embayment area (Figure 10). Secondly, the detachment of the terranes from the underlying craton allowed the section of craton northeast of the Shenandoah fault to be displaced northwestward by the Reguibat indentor beneath the terranes. Such underthrusting beneath the Paleozoic terranes during the Alleghanian is not the first to be noted along the Atlantic margin. The Avalon composite terrane in southern New England was underthrust beneath other Paleozoic terranes from Early Devonian through Early Permian times (e.g., Getty and Gromet, 1992; Wintsch and others, 1992).

Relationship Between the EC-SFS and Central Virginia Seismic Zone

The northwest-striking reverse faulting in the central Virginia seismic zone, as indicated by focal mechanisms (Bollinger and others, 1991), was perplexing because it crosscuts the northeast-trending structures in central Virginia (Figure 5B). Yet, the mapped, northeast-trending terrane boundaries display no significant northwest offsets. Thus, the cause of the seismicity remained enigmatic and led to various hypotheses regarding its origin, including reactivation of a preexisting zone of weakness (Sykes, 1978), hydroseismicity (Costain and others, 1987), and reactivated northeast-trending thrust faults (Çoruh and others, 1988).

In contrast to previous hypotheses, we postulate that the source of the seismicity may arise from intersecting northwest- and northeast-trending faults because the variation in fault plane orientations is like seismicity patterns at known fault intersections, like those near Summerville, South Carolina, and in the New Madrid seismic zone (e.g., Talwani, 1999) (Figure 11B and 11C). The Shenandoah fault is the best candidate for the northwest-trending structure. Because the Shenandoah fault apparently is a basement fault, the intersecting northeast-trending structure(s) also has to be a basement fault(s) to produce an intersection. Based on available seismic-reflection data, the northeast-trending, southeast-dipping Paleozoic faults within the allochthonous terranes in northern Virginia become listric at depth (e.g., Çoruh and

others, 1988) and, thus, would not be cut by the Shenandoah fault to produce a major fault intersection (Figure 6). A more likely scenario is that the EC-SFS is a reactivated basement fault system offset along the Shenandoah fault and that late Cenozoic dextral displacement on the EC-SFS is producing compression at the offset location (Figure 11A). The presence of north- to northeast-trending Cenozoic faults near the offset (Figure 3) is consistent with the hypothesis that some of them could be linking faults that have reconnected the EC-SFS along a left-step restraining bend (Figure 11A). This hypothesis is supported by their orientation and the cross-cutting relationship between several of these faults and the Paleozoic thrust faults (e.g., Hylas mylonite zone) and Triassic basin faults (Marple, 2004). The Port Royal fault and the Cenozoic faults west of the basin (Figure 3), for example, dip steeply to the west (Mixon and others, 1992) while the basin border fault and Hylas zone dip to the east (Milici and others, 1991; LeTourneau, 1999). A few of the Cenozoic faults, in contrast, appear to be associated with reactivated basin border faults, such as the southeast-dipping Brandywine fault and Skinkers Neck fault along the Taylorsville basin border.

Possible evidence for compressional uplift near the restraining bend is inferred from anomalously elevated James River terraces east of the Blue Ridge Province (Hancock and others, 2004). Also, note how the Fall Zone parallels the ECFS, Stafford fault, and Cenozoic faults between central North Carolina and Long Island (Figures 1 and 3). This observation suggests that the location of this part of the Fall Zone may have been influenced by long-term deformation on the EC-SFS. Thus, it is likely that the central Virginia seismicity is from compression produced by dextral displacement along the EC-SFS bend, which has reactivated a variety of nearby faults, including the linking faults, Shenandoah fault, and northeast-trending Paleozoic faults.

Possible Association of the Shenandoah Igneous Province with the EC-SFS and Shenandoah Fault

The Late Jurassic and middle Eocene intrusive rocks of the Shenandoah igneous province in western Virginia are unique because they are farther west than most Early Jurassic rift-related diabase dikes, they strike more northwesterly than the older diabase dikes north of southern Virginia (Figure 4A), and because the Eocene intrusive rocks are the youngest in the eastern U.S. (Southworth and others, 1993). Southworth and others (1993) attributed the Late Jurassic alkalic igneous dikes to reactivation of a cross-strike (northwest-trending) basement fault during Mesozoic extension. However, there are at least two arguments against this scenario. First, the approximately east-west extensional stress field that produced the north-northwest-trending Early Jurassic dikes just to the east (Figure 4A) would have favored transtension on the Shenandoah basement fault and, thus, magmatic activity in the Shenandoah province during Early Jurassic time. Yet, there are no such igneous features in the province. Secondly, rift-related extension in the mid-Atlantic states ended before intrusion of the Late Jurassic dikes. Based on the northeast and northwest trends of many Eocene dikes in the province, Southworth and others (1993) attributed the Eocene intrusive rocks to rapid emplacement through northwest- and northeast-trending basement faults that were extensionally reactivated during a change in plate motion from 53.5 to 37.5 Ma (Vogt, 1991). However, the local nature of these igneous intrusive rocks suggests that they are associated with a local process rather than regional extension.

The overall northwest elongation of the igneous province and the normal fault on the seismic-reflection profile (Figure 4) support the presence of a northwest-oriented basement fault zone beneath the Valley and Ridge strata, which we postulate is the Shenandoah fault. Normal-sense faulting in the Shenandoah province during Late Jurassic and middle Eocene times is perplexing, though, because there is no evidence for a regional northeast-oriented exten-

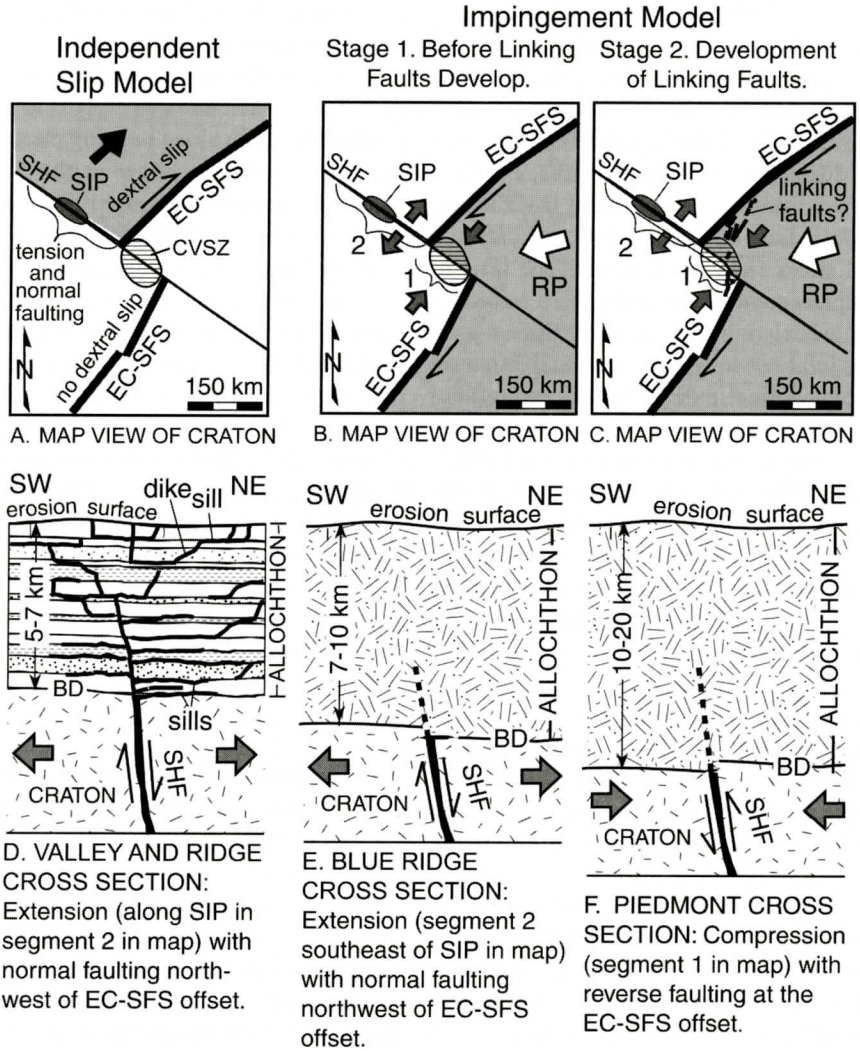

Figure 12. Conceptual models illustrating two possible origins of the Shenandoah igneous province (SIP, gray elliptical area in diagrams A-C). Diagrams A-C are map views of the craton without the overlying allochthonous terranes. In diagram A, the crust northeast of the Shenandoah fault (SHF) and west of the EC-SFS (shaded area) slipped northeastward during Late Jurassic and middle Eocene times, independent of the crust southwest of the SHF, thus producing tension and normal faulting on the SHF to the northwest. In the second model, ridge push forces (RP) from the east-northeast (large open arrows, diagrams B and C) caused the craton east of the EC-SFS (shaded) to move southwest relative to the craton to the west (unshaded) during Late Jurassic and middle Eocene times. Consequently, the craton east of the EC-SFS impinged on the craton to the west along segment 1 (EC-SFS offset) of the SHF. This impingement caused compression (striped area) and reverse-sense reactivation of the SHF along segment 1 (diagram F) and forced apart the SHF to the northwest (segment 2), causing normal-sense reactivation of the SHF to the northwest. Linking faults may have developed across the offset (diagram C) as compression and impingement continued at segment 1 (diagrams C and F). Magma (thick black lines in cross section D) migrated up the SHF and then along bedding planes and preexisting northwest joints. Diagram E demonstrates how the magmas might not have been able to migrate upward through the crystalline Blue Ridge-Piedmont rocks. BD, basal decollement; CVSZ, central Virginia seismic zone.

sional stress field along the U.S. Atlantic margin during these times. Studies of the Stafford fault zone (Mixon and others, 1992), for example, support east- to northeast-oriented compression along the middle U.S. Atlantic margin during middle Eocene time. Furthermore, the northwest orientation of the Shenandoah dikes does not necessarily indicate the regional stress field orientation at the time of their emplacement. These dikes were emplaced along a preexisting Paleozoic northwest joint set. This joint set, in which individual joints are of limited vertical extent, occurs throughout much of the Appalachians. Yet, the Shenandoah igneous province is confined to a relatively small area. This observation contrasts with the emplacement of Early Jurassic dikes throughout the eastern U.S. along extensional fractures produced by early Mesozoic rifting. Thus, the cause of the normal faulting and igneous activity in the Shenandoah province is most likely local.

Our investigation suggests that the cause of the normal faulting may have involved interactions between the EC-SFS and Shenandoah fault in central Virginia. Because both periods of igneous activity coincided with two major dextral strike-slip shear phases in the Appalachians at about 155-147 and 47-38 Ma (e.g., de Boer and others, 1988), we hypothesize that dextral movement on the EC-SFS in central Virginia during Late Jurassic and middle Eocene times could have caused local tension and normal-sense displacement on the Shenandoah fault to the northwest beneath the allochthonous terranes of the Valley and Ridge and Blue Ridge provinces (Figure 12). One possible scenario is that the crust north of the Shenandoah fault and west of the EC-SFS moved northeastward, independent of the crustal block to the southwest. This mechanism could have produced tension and normal faulting on the Shenandoah fault northwest of the EC-SFS offset (Figure 12A). Another possible model involves the southwest movement of the crust east of the EC-SFS relative to the crust to the west (Figures 12B and 12C). This relative motion caused the crust to the east to impinge on the crust west of the offset, thus forcing apart the Shenandoah fault to the northwest and causing tension and normal faulting.

The normal-sense reactivation of the Shenandoah fault allowed magma to migrate up the fault and then along bedding planes and preexisting northwest joints in the Valley and Ridge strata (Figures 4B and 12D). The absence of dikes along the Shenandoah fault trend in the Blue Ridge Province to the southeast (Figure 4A) suggests that the magmas were unable to migrate upward through the overlying Blue Ridge igneous and metamorphic rocks. The impenetrability of these crystalline Blue Ridge rocks is a function of their greater thickness (Figure 12E), their lower anisotropy, general composition (e.g., water content), and their higher tensile strength (Touloukian and others, 1981) compared to the Valley and Ridge sedimentary rocks. Variations in chemistry and thermodynamics of the mantle and lower crust along the Shenandoah fault also may have contributed to localization of the igneous intrusives.

Northeast/Southwest-Oriented Extension Northwest of the Indention

Based on a study of regional cross-fold joints in the northern Allegheny Plateau, Zhao and Jacobi (1997) postulated that northwest-directed compression from the Reguibat indentor produced northeast/southwest-oriented extension to the northwest in the Valley and Ridge and Allegheny Plateau provinces. Longer, northwest-trending lineaments in Pennsylvania and surrounding states may also represent evidence for extension northwest of the zone of indention. These lineaments include the Pittsburgh-Washington (PW), Tyrone-Mt. Union (TMU), and other unnamed lineaments (Lavin and others, 1982) (Figure 9). They are generally defined by an increase in northwest-trending joint density, a series of fold terminations, and aligned drainage patterns and water gaps (e.g., Rodgers and Anderson, 1984). Lavin and others (1982) suggested that the lineaments represent locations of pre-Alleghanian basement cross faults and that as much as 60 km of shear may have occurred

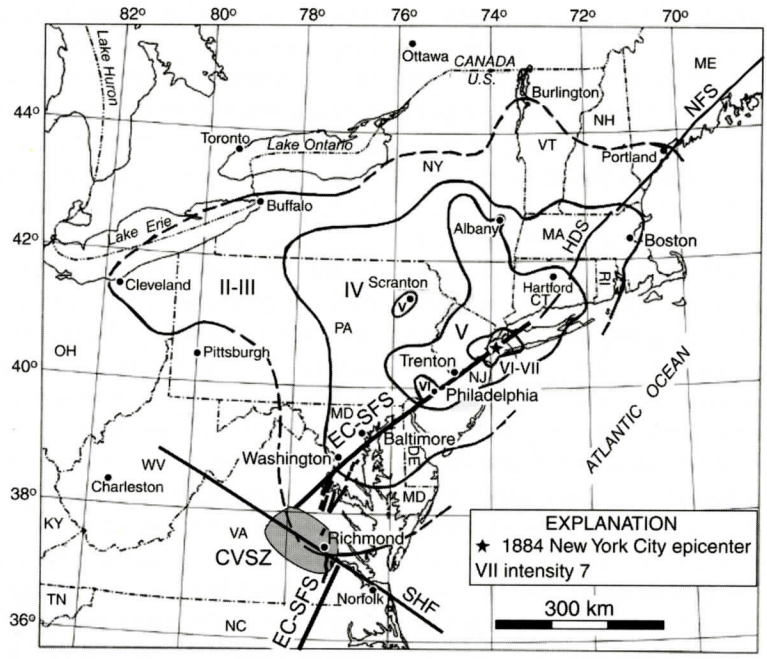

Figure 13. Comparison of the EC-SFS with the isoseismals of the 1884 New York City earthquake (M ~5.5) (closed contours). Also shown are Cenozoic faults from Figure 3 which could be linking faults. CVSZ, central Virginia seismic zone; HDS, Higggganum dike system; NFS, Norumbega fault system; SHF, Shenandoah fault. Modified from Stover and Coffman (1993).

on the PW and TMU lineaments. Rodgers and Anderson (1984), however, argued against shearing along the TMU lineament. They postulated that the lineaments were produced by Alleghanian normal-sense reactivation of basement faults by northeast-oriented extension orthogonal to the northwest-oriented compression along the continental-collision zone. The northeast extension was likely produced by northwest-oriented compression in the Salisbury embayment and Piedmont areas by the Reguibat indentor (Figure 9). This hypothesis is supported by at least two observations: (1) the coincidence of Alleghanian northwest-trending normal-sense faulting (Tipton block) with the TMU lineament near the Allegheny front in central Pennsylvania (Faill, 1981) and (2) the parallelism between the PW and TMU lineaments and the Shenandoah fault (Figure 9). Such extensional stress conditions exist in Tibet north of the Himalayan continental-collision zone, where the crust is stretched in a direction generally orthogonal to the convergence direction (e.g., Zoback and others, 1989).

Late Cenozoic Deformation and Seismic Potential of the EC-SFS

Several observations indicate that late Cenozoic deformation has occurred on the EC-SFS. First, the coincidence of the southern end of the EC-SFS with the highest intensity isoseismals of the 1886 Charleston, South Carolina, earthquake strongly suggests that this segment broke in 1886 (Marple and Talwani, 2000). There is also evidence for historical, small- to moderate-sized earthquakes along various parts of the Stafford segment between central Virginia and New York City (Marple, 2004). The alignment of the EC-SFS with the highest intensity isoseismals of the 1884 New York City earthquake, for example, suggests that it could have caused this earthquake (Figure 13). Secondly, paleoseismic data suggest that several prehistoric M7+ earthquakes occurred in the Charleston region and that one M6+ earthquake occurred

about 100 km north of Charleston at ~1500 B.P. (Talwani and Schaeffer, 2001), the source of which may be the EC-SFS. Third, surface faults offsetting Pliocene- to Pleistocene-age sediments in central North Carolina and anomalous changes in river morphology along most of its length indicate that late Pliocene to Holocene deformation has occurred on the EC-SFS (Marple and Talwani, 2000; Marple, 2004). Yet, the EC-SFS currently displays low-level seismicity, even south of Summerville where it likely broke in 1886. This low-level seismicity can be explained in at least six ways: 1) segments of the EC-SFS are intermittently active with periods of little or no activity between moderate to large earthquakes, 2) the EC-SFS is undergoing aseismic creep, 3) segments that have produced large earthquakes in the past are presently locked with strain accumulating, 4) the present stress field is not optimally oriented to produce major seismicity, 5) the absence of suitably oriented cross-faults, and 6) by the low strain rate in the eastern U.S.

The first scenario suggests that segments of the EC-SFS could be in a period of little or no deformation between earthquakes. It has been postulated, for example, that faults in other intraplate areas are intermittently active between periods of little or no deformation, such as those that have produced historic earthquakes in Australia (e.g., Machette and others, 1993), the Bootheel fault in the New Madrid region (Guccione and others, in press), and the Meers fault in Oklahoma (Crone and Luza, 1990), the latter two of which are nearly aseismic at present. Also, as mentioned previously, the EC-SFS segment that probably broke in 1886 south of Summerville is nearly aseismic (Marple and Talwani, 2000).

It is also possible that certain segments of the EC-SFS are currently locked. The large restraining bend in the EC-SFS is especially intriguing because it probably affects the timing and magnitude of lateral displacements on the EC-SFS and because it is a likely site of strain accumulation (Talwani, 1999), as suggested by the central Virginia seismicity and the anomalously elevated James River terraces (Hancock and others, 2004). Examples of locked, currently aseismic faults that have produced large historic earthquakes include the large segments of the San Andreas fault that ruptured in 1857 and 1906 (Wallace, 1990). Thus, the low-level seismicity along much of the EC-SFS does not necessarily indicate that it is inactive or that it could not produce large earthquakes in the future.

Seismicity and fault slip rate are also affected by the stress field orientation relative to faults (Sibson, 1990). The EC-SFS in South Carolina north of Summerville, for example, is favorably oriented for dextral displacement relative to the orientation of maximum horizontal compressive stress (Marple and Talwani, 2000). However, most of the fault system there is currently aseismic, except near Summerville. Thus, stress field orientation does not account for the low-level seismicity along this part of the EC-SFS. The stress field orientation near the rest of the EC-SFS is difficult to determine. Near the EC-SFS in eastern North Carolina and between Long Island and Delaware, there are little or no stress data (Zoback and Zoback, 1991). Between Virginia and Delaware, in contrast, there is a large variation in stress axis orientations. Near the EC-SFS in Virginia, for example, the stress axis orientations range from moderate to high angles relative to the EC-SFS while stress axes offshore and to the west are at low angles to the EC-SFS (Zoback and Zoback, 1991). Thus, the affect of stress field orientation on the EC-SFS will be difficult to evaluate until there are more stress data between North Carolina and New Jersey.

Based on these observations and the likelihood that its southern end produced the 1886 Charleston, South Carolina, earthquake, the EC-SFS should be further investigated to determine if other segments could someday produce large damaging earthquakes like the 1886 event. The greatest potential for damage from a large earthquake is along the EC-SFS between Richmond, Virginia, and New York City where there are several large population centers near its trend (Figure 13).

CONCLUSIONS AND SUMMARY

Our results have tectonic implications for the

eastern U.S. for several reasons. First, they help to refine the nature of Alleghanian indention in the Salisbury embayment area. Secondly, they provide an explanation for the origin of several, previously enigmatic features, including the central Virginia seismic zone and Shenandoah igneous province. The following summary highlights our results.

The Shenandoah igneous province, central Virginia seismic zone, and a northwest-trending linear magnetic anomaly offshore Virginia appear to be associated with a deep-crustal, northwest-trending Shenandoah basement fault. The fact that the Shenandoah fault, ECFS, and Stafford fault crosscut the southeast-dipping Paleozoic allochthonous terranes and structures suggests that they are basement faults.

The following sequence of events likely occurred in the evolution of these fault systems. Before late Alleghanian indention, the Stafford fault zone and ECFS were a continuous, deep-crustal strike-slip fault system. During the Alleghanian or an earlier orogeny, the East Coast-Stafford fault system (EC-SFS) was beheaded by westward thrusting of the allochthonous terranes, thus concealing its ductile roots. During late Alleghanian head-on (northwest) collision, indention in the Salisbury embayment area by the Reguibat uplift of northwest Africa created the Shenandoah fault and offset the EC-SFS left-laterally beneath the allochthonous terranes. Late Jurassic to Cenozoic dextral reactivation of the EC-SFS ductile roots fractured the overlying allochthonous terranes and may have produced north- to northeast-oriented linking faults across the central Virginia offset that have reconnected the EC-SFS along a large restraining bend. Late Cenozoic dextral displacement on the EC-SFS across the bend has reactivated the linking faults, Shenandoah fault, and other faults in central Virginia, thus producing the central Virginia seismic zone.

Late Jurassic and middle Eocene dextral displacement on the EC-SFS in the vicinity of the central Virginia bend may have produced tension and normal-sense displacement on the Shenandoah fault to the northwest beneath the allochthonous terranes. Consequently, magma migrated up the Shenandoah fault and then along bedding planes and joints in the Valley and Ridge thrust sheet complex, locally crosscutting strata, to produce the Shenandoah igneous province in western Virginia.

ACKNOWLEDGMENTS

Acknowledgment is made to Seismic Exchange of Houston, Texas for allowing us to use their seismic-reflection data and to Geosignal (Division of WesternGeco) in Houston, Texas for permitting us to use their computer software and facilities to process the data. Our appreciation is extended to Kevin Stewart, Loren Raymond, and Peter Malin for their critical reading of this manuscript. We also thank Robert Hatcher for his helpful comments.

REFERENCES CITED

Badley, M.E., 1985, Practical seismic interpretation: Prentice-Hall, Englewood Cliffs, New Jersey, 266 p.

Behrendt, J.C., and Grim, M.S., 1985, Structure of the U.S. Atlantic continental margin from derivative and filtered maps of the magnetic field, *in* Hinze, W.J., ed., The utility of regional gravity and magnetic anomaly maps: Tulsa, Oklahoma, Society of Exploration Geophysicists, p. 325-338.

Benson, R.N., 1992, Map of exposed and buried early Mesozoic rift basins/synrift rocks of the U.S. middle Atlantic continental margin: Delaware Geological Survey Miscellaneous Map Series No. 5, scale 1:1 000 000, 1 sheet.

Bollinger, G.A., Johnston, A.C., Talwani, P., Long, L.T., Shedlock, K.M., Sibol, M.S., and Chapman, M.C., 1991, Seismicity of the southeastern United States; 1698 to 1986, *in* Slemmons, D.B., Engdahl, E.R., Zoback, M.D., and Blackwell, D.D., eds., Neotectonics of North America: Boulder, Colorado, Geological Society of America, Decade Map Volume 1, p. 291-308.

Bramlett, K.W., Secor, W.D., and Prowell, D.C., 1982, The Belair fault: A Cenozoic reactivation structure in the eastern Piedmont: Geological Society of America Bulletin, v. 93, p. 1109-1117

Cederstrom, K.J., 1945, Structural geology of southeastern Virginia: American Association of Petroleum Geologists Bulletin, v. 29, no. 1, p. 71-95.

Çoruh, C., Bollinger, G.A., and Costain, J.K., 1988, Seismogenic structures in the central Virginia seismic zone: Geology, v. 16, p. 748-751.

Costain, J.K., Bollinger, G.A., and Speer, J.A., 1987, Hydroseismicity — A hypothesis for the role of water in the generation of intraplate seismicity: Seismological Research Letters, v. 58, no. 3, p. 41-64.

Crone, A.J., and Luza, K.V., 1990, Style and timing of Holocene surface faulting on the Meers fault, south-

western Oklahoma: Geological Society of America Bulletin, v. 102, p. 1-17.

de Boer, J.Z., McHone, J.G., Puffer, J.H., Ragland, P.C., and Whittington, D., 1988, Mesozoic and Cenozoic magmatism, *in* Sheridan, R.E., and Grow, J.A., eds., The Atlantic continental margin, U.S.: Boulder, Colorado, Geological Society of America, Geology of North America, v. I-2, p. 217-241.

Deynoux, M., Sougy, J., and Trompette, R., 1982, Lower Palaeozoic rocks of west Africa and the western part of central Africa, *in* von Rad, U., Hinz, K., Sarnthein, M., and Seibold, E., eds., Geology of the northwest African continental margin 3: New York, Springer-Verlag, p. 337-392.

Faill, R.T., 1981, The Tipton Block; An unusual structure in the Appalachians: Pennsylvania Geology, v. 12, no. 2, p. 5-9.

Fletcher, J.B., Sbar, M.L., and Sykes, L.R., 1978, Seismic trends and travel time residuals in eastern North America and their tectonic implications: Geological Society of America Bulletin, v. 89, p. 1656-1676.

Fullagar, P.D., and Bottino, M.L., 1969, Tertiary felsite intrusions in the Valley and Ridge province, Virginia: Geological Society of America Bulletin, v. 80, p. 1853-1858.

Gangopadhyay, A., and Talwani, P., 2003, Symptomatic features of intraplate earthquakes: Seismological Research Letters, v. 74, p. 863-883.

Geologic Map of Virginia, 1993, Virginia Division of Mineral Resources, scale 1:500 000, 1 sheet.

Getty, S.R., and Gromet, L.P., 1992, Evidence for extension at the Willimantic Dome, Connecticut; Implications for the Late Paleozoic tectonic evolution of the New England Appalachians: American Journal of Science, v. 292, p. 398-420.

Glover, L., III, Sheridan, R.E., Holbrook, W.S., Ewing, J., Talwani, M., Hawman, R.B., and Wang, P., 1997, Paleozoic collisions, Mesozoic rifting, and structure of the Middle Atlantic states continental margin: An 'EDGE' Project report: *in* Glover, L., III, and Gates, A.E., eds., Central and Southern Appalachian Sutures: Results of the EDGE Project and Related Studies: Boulder, Colorado, Geological Society of America Special Paper 314, p. 107-135.

Guccione, M., Marple, R., and Autin, W. [in press], Evidence for Holocene displacements along the Bootheel fault (lineament) in southeastern Missouri: Seismotectonic implications for the New Madrid Region: Geological Society of America Bulletin.

Hack, J.T., 1989, Geomorphology of the Appalachian Highlands: *in* Hatcher, R.D., Jr., Thomas, W.A., and Viele, G.W., eds., The Appalachian-Quachita Orogen in the United States: Geological Society of America, The Geology of North America, v. F-2, p. 459-470.

Hancock, G.S., Harbor, D.J., Felis, J., and Turcotte, J., 2004, ^{10}Be dating of river terraces reveals Piedmont landscape disequilibrium in the central James River basin, Virginia: Geological Society of America Abstracts with Programs, v. 36, no. 2, p. 95.

Harris, L.D., and Milici, R.C., 1977, Characteristics of thin-skinned style of deformation in the southern Appalachians, and potential hydrocarbon traps: U.S. Geological Survey Professional Paper 1018, 40 p.

Hatcher, R.D., Jr., 1989, Tectonic synthesis of the U.S. Appalachians, *in* Hatcher, R.D., Jr., Thomas, W.A., and Viele, G.W., eds., The Appalachian-Quachita orogen in the United States: Boulder, Colorado, Geological Society of America, Geology of North America, v. F-2, p. 511-535.

Hatcher, R.D., Jr., 2002, Alleghanian (Appalachian) orogeny, a product of zipper tectonics: Rotational transpressive continent-continent collision and closing of ancient oceans along irregular margins, *in* Martínez Catalán, J.R., Hatcher, R.D., Jr., Arenas, R., and Díaz García, F., eds., Variscan-Appalachian dynamics: Boulder, Colorado, Geological Society of America Special Paper 364, p. 199-208.

Hatcher, R.D., Jr., Howell, D.E., and Talwani, P., 1977, Eastern Piedmont fault system: Speculations on its extent: Geology, v. 5, p. 636-640.

Hatcher, R.D., Jr., Thomas, W.A., Geiser, P.A., Snoke, A.W., Mosher, S., and Wiltschko, D.V., 1989, Alleghanian orogen, *in* Hatcher, R.D., Jr., Thomas, W.A., and Viele, G.W., eds., The Appalachian-Quachita orogen in the United States: Boulder, Colorado, Geological Society of America, Geology of North America, v. F-2, p. 233-318.

Johnston, A.C., Reinbold, D.J., and Brewer, S.I., 1985, Seismotectonics of the southern Appalachians: Seismological Society of America Bulletin, v. 75, p. 291-312.

King, E.R., and Zietz, I., 1978, The New York-Alabama lineament: Geophysical evidence for a major crustal break in the basement beneath the Appalachian basin: Geology, v. 6, p. 312-318.

Klitgord, K.D., and Schouten, H., 1986, Plate kinematics of the central Atlantic, *in* Vogt, P.R., and Tucholke, B.E., eds., The western North Atlantic region: Boulder, Colorado, Geological Society of America, Geology of North America, v. M, p. 351-378.

Klitgord, K.D., Poag, C.W., Schneider, C.M., and North, L., 1994, Geophysical database of the east coast of the United States northern Atlantic margin: Cross sections and gridded database: U.S. Geological Survey Open File Report 94-637, 188 p.

Krohn, M.D., and Phillips, J.D., 1982, A principal component enhancement for Landsat images: Possible structural applications in vegetated Virginia Piedmont: American Association of Petroleum Geologists, v. 66, no. 5, p. 590 (abstract).

Lavin, P.M., Chaffin, D.L., and Davis, W.F., 1982, Major lineaments and the Lake Erie-Maryland crustal block: Tectonics, v. 1, no. 5, p. 431-440.

Lécorché, J.P., Roussel, J., and Sougy, J., 1983, An interpretation of the geology of the Mauritanides orogenic belt (West Africa) in the light of geophysical data, *in* Hatcher, R.D., Jr., Williams, H., and Zietz, I., eds., Con-

tributions to the tectonics and geophysics of mountain chains: Geological Society of America Memoir 158, p. 131-147.

Lefort, J.P., 1988, Imprint of the Reguibat uplift (Mauritania) on the central and southern Appalachians of the U.S.A.: Journal of African Earth Sciences, v. 7, no. 2, p. 433-442.

Lefort, J.P., and Max, M.D., 1991, Is there an Archean crust beneath Chesapeake Bay?: Tectonics, v. 10, no. 1, p. 213-226.

LeTourneau, P.M., 1999, Depositional history and tectonic evolution of Late Triassic age rifts of the U.S. central Atlantic margin: Results of an integrated stratigraphic, structural, and paleomagnetic analysis of the Taylorsville and Richmond basins [Ph.D. dissertation]: New York, Columbia University, 294 p.

Machette, M.N., Crone, A.J., and Bowman, J.R., 1993, Geologic investigations of the 1986 Marryat Creek, Australia, earthquake-implications for paleoseismicity in stable continental regions: U.S. Geological Survey Bulletin 2032-B, 29 p.

Madabhushi, S., and Talwani, P., 1993, Fault plane solutions and relocations of recent earthquakes in Middleton Place Summerville seismic zone near Charleston, South Carolina: Seismological Society of America Bulletin, v. 83, no. 5, p. 1442-1466.

Marple, R.T., 2004, Relationship of the Stafford fault zone to the right-stepping bends of the Potomac, Susquehanna, and Delaware Rivers and related upstream incision along the U.S. Mid-Atlantic Fall Line: Southeastern Geology, v. 42, p. 123-144.

Marple, R.T., and Talwani, P., 2000, Evidence for a buried fault system in the Coastal Plain of the Carolinas and Virginia–Implications for neotectonics in the southeastern United States: Geological Society of America Bulletin, v. 112, no. 2, p. 200-220.

Milici, R.C., Bayer, K., Pappano, P.A., Costain, J.K., Çoruh, C., and Nolde, J.E., 1991, Preliminary geologic section across the buried part of the Taylorsville basin, Essex and Caroline counties, Virginia: Virginia Division of Mineral Resources Open File Report 91-1, 31 p.

Mixon, R.B., and Newell, W.L., 1977, Stafford fault system–Structures documenting Cretaceous and Tertiary deformation along the Fall Line in northeastern Virginia: Geology, v. 5, no. 7, p. 437-440.

Mixon, R.B., Berquist, C.R., Jr., Newell, W.L., Johnson, G.H., Powars, D.S., Schindler, J.S., and Rader, E.K., 1989, Geologic map and generalized cross sections of the Coastal Plain and adjacent parts of the Piedmont, Virginia: U.S. Geological Survey Miscellaneous Investigation Series Map I-2033, scale 1:250 000, 2 sheets.

Mixon, R.B., Powars, D.S., and Daniels, D.L., 1992, Nature and timing of deformation of Upper Mesozoic and Cenozoic deposits in the inner Atlantic Coastal Plain, Virginia and Maryland, *in* Gohn, G.S., ed., Proceedings of the 1988 U.S. Geological Survey Workshop on the Geology and Geohydrology of the Atlantic Coastal Plain: U.S. Geological Survey Circular 1059, p. 65-73.

Powars, D.S., and Bruce, T.S., 1999, The effects of the Chesapeake Bay impact crater on the geological framework and correlation of hydrogeologic units of the lower York-James Peninsula, Virginia: U.S. Geological Survey Professional Paper 1612, 7 plates, 82 p.

Rader, E.K., and Wilkes, G.P., 2001, Geologic map of Virginia portion of the Staunton 30 x 60 minute quadrangle: Virginia Division of Mineral Resources, Geologic Map no. 163, scale 1:100 000, 1 sheet.

Rodgers, M.R., and Anderson, T.H., 1984, Tyrone-Mt. Union cross-strike lineament of Pennsylvania: A major Paleozoic basement fracture and uplift boundary: American Association of Petroleum Geologists Bulletin, v. 68, no. 1, p. 92-105.

Sbar, M.L., Jordan, R.R., Stephens, C.D., Pickett, T.E., Woodruff, K.D., and Sammis, C.G., 1975, The Delaware-New Jersey earthquake of February 28, 1973: Seismological Society of America Bulletin, v. 65, p. 85-92.

Sheridan, R.E., Maguire, T.J., Feigenson, M.D., Patino, L.C., and Volkert, R.A., 1999, Grenville age of basement rocks in Cape May NJ well: New evidence for Laurentian crust in U.S. Atlantic Coastal Plain basement Chesapeake Terrane: Journal of Geodynamics: v. 27, p. 623-633.

Sibson, R.H., 1990, Rupture nucleation on unfavorably oriented faults: Bulletin of the Seismological Society of America, v. 80, no. 6, p. 1580-1604.

Southworth, C.S., Gray, K.J., and Sutter, J.F., 1993, Middle Eocene intrusive igneous rocks of the central Appalachian Valley and Ridge province — Setting, chemistry, and implications for crustal structure: U.S. Geological Survey Bulletin 1839-J, p. J1-J24.

Stover, C.W., and Coffman, J.L., 1993, Seismicity of the United States, 1568-1989, (revised), U.S. Geological Survey Professional Paper 1527, 418 p.

Sykes, L.R., 1978, Intraplate seismicity, reactivation of preexisting zones of weakness, alkaline magmatism, and other tectonism postdating continental fragmentation: Reviews of Geophysics and Space Physics, v. 16, p. 621-687.

Talwani, P., 1999, Fault geometry and earthquakes in continental interiors: Tectonophysics, v. 305, p. 371-379.

Talwani, P., and Schaeffer, W.T., 2001, Recurrence rates of large earthquakes in the South Carolina Coastal Plain based on paleoliquefaction data: Journal of Geophysical Research, v. 106, p. 6621-6642.

Tapponnier, P., Zhiqin, X., Roger, F., Meyer, B., Arnaud, N., Wittlinger, G., and Jingsui, Y., 2001, Oblique stepwise rise and growth of the Tibet Plateau: Science, v. 294, p. 1671-1677.

Toft, P.B., Taylor, P.T., Arkani-Hamed, J., and Haggerty, S.E., 1992, Interpretation of satellite magnetic anomalies over the West African Craton: Tectonophysics, v. 212, p. 21-32.

Touloukian, Y.S., Judd, W.R., and Roy, R.F., eds., 1981, Physical properties of rocks and minerals: New York, McGraw-Hill, CINDAS Data Series on Material Prop-

erties, v. II-2, 548 p.

Tso, J.L., McDowell, R.R., Avary, K.L., Matchen, D.L., and Wilkes, G.P., 2004, Middle Eocene igneous rocks in the Valley and Ridge of Virginia and West Virginia: *in* Southworth, S., and Burton, W., eds., Geology of the national capital region-field trip guidebook: U.S. Geological Survey Circular 1264, p. 136-161.

Vauchez, A., Kessler, S.F., Lécorché, J.P., and Villeneuve, M., 1987, Southward extrusion tectonics during the Carboniferous Africa–North America collision: Tectonophysics, v. 142, p. 317-322.

Vogt, P.R., 1991, Bermuda and Appalachian-Labrador rises: Common non-hotspot processes?: Geology, v. 19, no. 1, p. 41-44.

Wallace, R.E., 1990, The San Andreas fault system, ed., U.S. Geological Survey Professional Paper 1515, 279 p.

Weigel, W., Wissmann, G., and Goldflam, P., 1982, Deep seismic structure (Mauritania and central Morocco), *in* von Rad, U., Hinz, K., Sarnthein, M., and Seibold, E., eds., Geology of the northwest African continental margin 3: New York, Springer-Verlag, p. 132-159.

Wilkes, G.P., 1993, Mapped units of the Mesozoic basins, *in* Rader, E.K., and Evans, N.H., eds., Geologic map of Virginia — Expanded explanation: Virginia Division of Mineral Resources, p. 67-69.

Wintsch, R.P., Sutter, J.F., Kunk, M.J., Aleinikoff, J.N., and Dorais, M.J., 1992, Contrasting P-T-t paths: Thermochronologic evidence for a late Paleozoic final assembly of the Avalon composite terrane in the New England Appalachians: Tectonics, v. 11, p. 672-689.

Zhao, M., and Jacobi, R.D., 1997, Formation of regional cross-fold joints in the northern Appalachian Plateau: Journal of Structural Geology, v. 19, no. 6, p. 817-834.

Zoback, M.L., and Zoback, M.D., 1991, Tectonic stress field of North America and relative plate motions, *in* Slemmons, D.B., Engdahl, E.R., Zoback, M.D., and Blackwell, D.D., eds., Neotectonics of North America: Boulder, Colorado, Geological Society of America, Decade Map Volume 1, p. 339-366.

Zoback, M.L, Zoback, M.D., Adams, J., Assumpcao, M., Bell, S., Bergman, E.A., Blumling, P., Brereton, N.R., Denham, D., Ding, J., Fuchs, K., Gay, N., Gregersen, S., Gupta, H.K., Gvishiani, A., Jacob, K., Klein, R., Knoll, P., Magee, M., Mercier, J.L., Muller, B.C., Paquin, C., Rajendran, K., Stephansson, O., Suarez, G., Suter, M., Udias, A., Xu, Z.H., and Zhizhin, M., 1989, Global patterns of tectonic stress: Nature, v. 341, p. 291-298.

SOUTHEASTERN GEOLOGY
V. 43, No. 2, November 2004, p. 81-102

CHEMICAL CONSTITUENTS IN THE PEEDEE AND CASTLE HAYNE AQUIFERS: PORTERS NECK AREA, NEW HANOVER COUNTY, NORTH CAROLINA

TINA L. ROBERTS[1]

The Florida Geological Survey
903 W. Tennessee St.
Tallahassee, FL 32304

W. BURLEIGH HARRIS

Department. of Earth Sciences
University of North Carolina-Wilmington
Wilmington, NC 28401

1. Current address, EA Engineering, Science, and Technology, Inc., Anderson AFB-Guam, PO Box 4355, Yigo, Guam 96929-4355

ABSTRACT

Concerns about overuse and potential contamination of major aquifers in the southeastern part of North Carolina resulted in the initiation of a subsurface water quality study in February 2001. The focus of this study was to examine variations in nutrients (NO_3^-, TRP, SO_4^{2-}, Cl^-, NH_4^+) and total dissolved Fe in the Cretaceous Peedee and Tertiary Castle Hayne Limestone aquifers of northeastern New Hanover County. Water samples were collected monthly for one year from sixteen wells located in the Porters Neck area (west of the Intracoastal Waterway and south of Futch Creek) and four springs located on the south side of Futch Creek.

Variations in selective nutrient concentrations were measured between and within each aquifer. Concentrations of NH_4^+ and Fe increased in the Peedee sandstone aquifer during the warmer summer and early fall months. In late summer to early fall, Fe, NO_3^-, NH_4^+, and TRP concentrations in the Castle Hayne Limestone aquifer were significantly higher than in the spring and winter months. Chloride and SO_4^{2-} concentrations for the Castle Hayne Limestone aquifer both increased during the warmer months, probably as a result of saltwater intrusion.

Factors considered for nutrient and Fe variance include: temperature variation, anaerobic conditions, subsurface stratigraphy/structure, recharge locations, site location and surface fertilization. The shallower Castle Hayne Limestone aquifer showed seasonal variability in the study area, whereas the Peedee sandstone aquifer showed little to no seasonal variability. Increases in NO_3^- and TRP lagged slightly behind periods of high fertilization and were more prevalent down-dip of a major golf course. Nutrient content and seasonal variation of Futch Creek springs indicated that they originate from the Castle Hayne Limestone aquifer.

INTRODUCTION

Background

Recent water quality investigations of New Hanover County creeks that flow into the Atlantic Intracoastal Waterway show that concentrations of fecal coliforms, nutrients, and chlorophyll *a* are variable within individual systems as well as between systems (Mallin et al., 1998a). Over a four-year period, Futch Creek, located along the boundary between New Hanover and Pender County, showed the greatest variability in nutrient concentrations within the county, and the upper south branch of the creek consistently had higher concentrations of nutrients than other branches. In the summer and fall

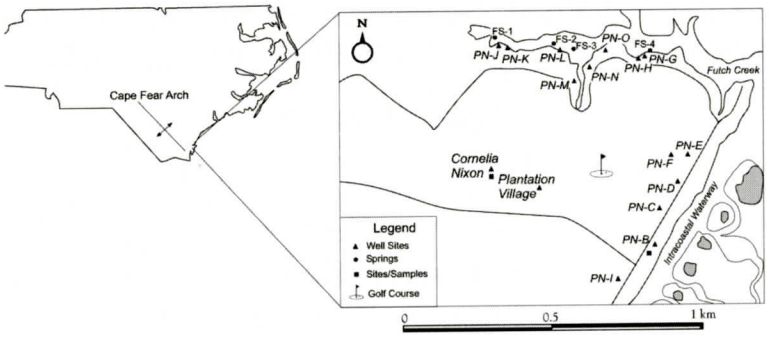

Figure 1. Porters Neck study area in northern New Hanover County, southeastern North Carolina. Sites where water samples were collected are illustrated as are sites where well samples were available for study.

of 1998 an intensive investigation was undertaken by Mallin et al. (1998b) to identify the potential sources of these nutrients to Futch Creek water. They discovered that Futch Creek was not only affected by shallow surface feeder creeks, but also by several freshwater springs located along the south side of the main channel. Although, Gramling (2003) quantified groundwater discharge to coastal waters using carbon and radium isotopes, no studies have identified the nutrients, determined the source of the springs, or their relationship to aquifers in the area.

The purpose of this paper is to determine the source for the springs, the nutrients present, and the nutrient budget for Futch Creek by examining aquifers in the Porters Neck area that are thought to be potential sources of water to the creek. As the two main aquifers in the area are the Peedee and Castle Hayne, the four main objectives are to 1) determine nutrient and dissolved Fe concentrations for the Peedee and Castle Hayne Limestone aquifers in the northeastern part of New Hanover County; 2) determine the relationship between the aquifers of the Porters Neck area and the fresh water springs located in Futch Creek; 3) examine nutrient and trace metal variability over time; and 4) determine the potential sources for each nutrient.

Study Area

The study area is the Porters Neck community of New Hanover County, a residential section composed largely of homes and extensive golf courses; it includes an area of about 12 sq. miles (Fig. 1). Futch Creek, a tidal creek located in this community, forms the boundary between New Hanover County and Pender County, and is located in the farthest southeastern part of the Coastal Plain Province of North Carolina. Water supplied in this area, either for potable or irrigational use, is derived from one of the three major aquifers by a personal well or a community water system. Residents or facilities that use the community water system also use a community sewer system. Those residents who rely on individual wells use septic tanks.

Individual wells obtain their water from one of the three aquifers that are associated with three different geologic units of different ages. These are the Late Cretaceous Peedee Formation, the Eocene Castle Hayne Limestone, and post-Miocene Surficial sands (Bain, 1970; Soil Survey of New Hanover County, North Carolina, 1977). Each aquifer varies in depth, structure, and sediment composition; therefore, the recharge rate and water composition varies for each. Recharge to these aquifers occurs by rainfall in the interstream areas, and by lateral inflow from areas located up-gradient of the study area (Lautier, 1998).

Recharge of the deeper aquifers, the Peedee and Castle Hayne aquifers occurs by water leaking downward from the Surficial aquifer, through the underlying confining beds in some areas. West of the study area, these units occur

on the surface and receive recharge by direct infiltration. The rate of recharge for these aquifers depends upon the difference in head values between the underlying aquifers and the Surficial aquifer, as well as the thickness and permeability of the confining beds (Lautier, 1998). The rate of recharge in the Peedee (thousands of years) and Castle Hayne Limestone aquifers (a few days to a few years) is significantly higher than the Surficial aquifer (usually a few days) due to variability in water velocities for each unit (Drever, 1997).

Twenty sites, 16 wells and four springs, were selected to conduct this study. Nine sites produced water from the Castle Hayne Limestone aquifer, seven sites produced water from the Peedee Formation aquifer, and four sites were freshwater springs located along the south side of Futch Creek (Fig.1). Well sites were distributed along Porters Neck Road, which parallels the south side of the Porters Neck Golf Course; Bald Eagle Lane, located east of the golf course and paralleling the Intracoastal Waterway; Futch Creek Road, located south and paralleling Futch Creek; as well as Creekside Lane and Saltwood Lane, two cul-de-sacs located at the south branch of Futch Creek (Fig. 1).

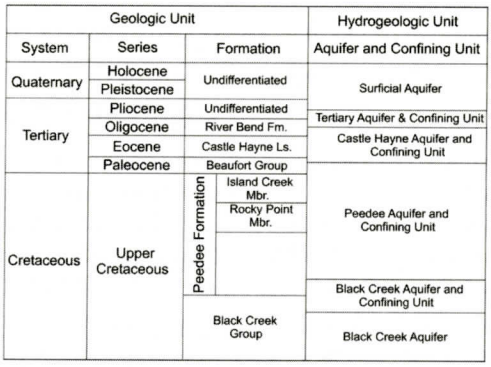

Figure 2. Generalized lithostratigraphy and hydrostratigraphy of Cretaceous, Tertiary and Quaternary units in southeastern North Carolina.

GEOLOGIC AND HYDROLOLOGIC SETTING

Stratigraphy

The study area lies on the north flank of a northwest-southeast trending positive feature known as the Cape Fear Arch (Fig. 1). A sequence of Cretaceous and Tertiary age sediments and sedimentary rocks occur in the area atop a southeast dipping basement of igneous and metamorphic rocks (Harris, 1998). Figure 2 illustrates the generalized stratigraphy of this area.

Cretaceous

The oldest sediments and sedimentary rocks in New Hanover County are assigned to the Upper Cretaceous Black Creek Group, and are known in southeastern North Carolina only from the subsurface. Lautier (1994) indicates that the altitude of the top of the Black Creek ranges between 94 m below sea level in western Brunswick County to 163 m below sea level in eastern New Hanover County. The Black Creek Group is composed of alternating beds of sand and clay that dip and thicken to the southeast. Inland, the Black Creek Group contains freshwater and is extensively used as a potable source for communities (Stehman, personal communication, 2002). However, in New Hanover County Bain (1970) indicates that sediments now assigned to the Black Creek Group only contain saline water. The Peedee Formation disconformably overlies the Black Creek Group, and because of the various features at the base of this formation, it is suggested that it is the result of ravinement without an extensive period of subaerial exposure (Harris, 1978). The Peedee Formation is composed of silty clay to very fine to fine clayey sand and ranges in depth from about 67 m below sea level to the surface in New Hanover County (Lautier, 1994). At the top of the Peedee Formation are two members, the older Rocky Point Member and the younger Island Creek Member (Dockal et al., 1998). Both members occur below Tertiary sediments and rocks depending upon location in the county. The Rocky Point Member ranges in thickness from zero to greater than 28 m. This unit is of limited lateral extent, and is found exclusively in northern New Hanover, eastern Pender, eastern Onslow and Brunswick Counties (Lautier, 1994). It is composed of cal-

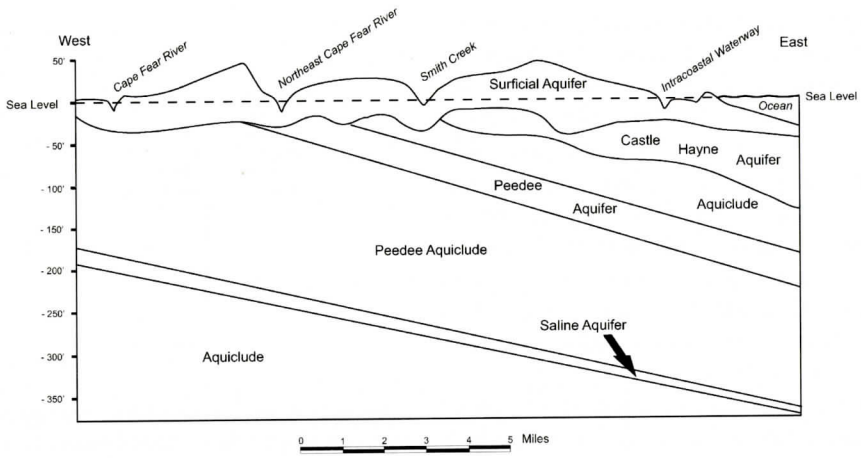

Figure 3. A generalized west-east cross-section of New Hanover County illustrating the major aquifers (section modified from Bain, 1970).

careous quartz arenite and sandy molluscan-rich grainstone. The Rocky Point Member is the most important aquifer in New Hanover County and is probably the Peedee Sandstone aquifer identified by Bain (1970). Above the Rocky Point Member of the Peedee Formation is the Island Creek Member, which consists of very fine to fine dolomitic clayey sand. Bain (1970) recognized an aquiclude (depth to +/- 60 m) above the Peedee Sandstone aquifer that most likely correlates to the Island Creek Member of Dockal et al. (1998) or the Beaufort Group.

Tertiary

The Castle Hayne Limestone crops out from the New Bern area of Craven County south to Brunswick County. Lautier (1994) states that the unit ranges from 4 m above sea level in southeastern Brunswick County to 40 m below sea level in the Carolina Beach area of New Hanover County. In the northern part of New Hanover County the Castle Hayne crops out on the Northeast Cape Fear River. In addition, several exposures also are identified along Burnt Mill Creek in the city of Wilmington (Lautier, 1994). The Castle Hayne Limestone disconformably overlies either the Rocky Point or Island Creek Member of the Peedee Formation in the northern part of New Hanover County. Its lithology varies from a basal phosphate pebble conglomerate, to dense limestone, to coarse shell-rich zones with high porosity and permeability. On top of the Castle Hayne Limestone is a sequence of sandy carbonate referred to as the River Bend Formation. This unit is Oligocene in age, disconformable on the Castle Hayne, and consists of soft silty to sandy lime mud or lithified sandy molluscan-mold limestone. Oligocene sediments and rocks are restricted to the subsurface area along and east of the Intracoastal Waterway in northern New Hanover County. Above the River Bend Formation are undifferentiated sand, clay, and organic-rich sediments varying in age from Pliocene to Recent that is grouped into Surficial deposits (Harris, 1998).

Aquifers

The three major fresh water-bearing hydrostratigraphic units occurring in New Hanover County are displayed in Figure 3. These units are the Peedee Sandstone aquifer, the Castle Hayne Limestone aquifer, and the Surficial aquifer.

Peedee Sandstone Aquifer

The lowermost aquifer is identified by Bain (1970) as a sandstone aquifer occurring in the Peedee Formation; it probably represents most of the lithostratigraphic Rocky Point Member. The Peedee sandstone aquifer ranges between 12 m above sea level in northeastern Brunswick

County to 67 m below sea level in southern New Hanover County. The aquifer has an average hydraulic conductivity of 12 m/day and an average transmissivity of 999 m^2/day (Lautier, 1994). The Peedee sandstone aquifer consists of gray or light brown, silty, fine to very fine grained quartz sand with trace quantities of glauconite, phosphorite, oyster shells, and pyrite (Lautier, 1998). In some areas the Peedee sandstone aquifer consists of gray, sandy, moldic limestone, grading downward to a zone of very calcareous sandstone. Below this unit lies a silt and clay aquiclude, and above it is a clay aquiclude of the Island Creek Member (Dockal et al., 1998; Harris, 1998). In southern New Hanover County, Paleocene sediments of the Beaufort Group also form an aquiclude above the sand.

Castle Hayne Limestone Aquifer

Overlying the Peedee Formation are the Castle Hayne Limestone and the River Bend Formation. These units comprise the single most productive aquifer in the North Carolina Coastal Plain, and are referred to as the Castle Hayne Limestone aquifer system (Harris, 1998). The Castle Hayne Limestone aquifer is absent in western Brunswick County and northwestern New Hanover County. It ranges to over 24 m in thickness in southern New Hanover County and has an average hydraulic conductivity of 11 m/day and an average transmissivity of 866 m^2/day (Lautier, 1994). The aquifer consists of light gray or white moldic limestones and bryozoan-rich limestones that grade in the deeper subsurface to calcareous fine grained sandstone (Lautier, 1998). In the east, it is overlain by a clay aquiclude; however, in the west where the aquiclude is not present, it may be connected to the Surficial aquifer. Also, to the west where the Island Creek Member and the Beaufort Group are missing, the Castle Hayne Limestone aquifer may be connected to the Peedee Sandstone aquifer, as there is no confining unit to separate the two aquifer systems. Limestones have substantial storage and very high permeabilities because of solution channels or fractures (Drever, 1997). In the study area, sinkholes have formed in the Castle Hayne Formation due to dissolution of the limestone by groundwater, thus causing hydraulic connection with overlying units (Lautier, 1994).

Surficial Aquifer

The Surficial aquifer, or unconfined aquifer, is present throughout New Hanover County, but it varies in form and shape with existing topography. The average hydraulic conductivity for this aquifer is 40 m/day and the average transmissivity is 850 m^2/day. This aquifer was once the primary source of water to county residents, but with rapid growth of the community during the past 20 years, its use for potable water has decreased. However, it is frequently used by county residents for irrigation (Lautier, 1998). In New Hanover County the Surficial aquifer provides storage and recharge that are important for the Castle Hayne beneath it.

METHODS

An area between Futch Creek to the north, the Intracoastal Waterway to the east, and a drainage divide to the south, was established as the study area (Fig. 1). On the basis of topography, this area is identified as being within the groundwater flow regime that includes the springs that eventually impact the surface waters of Futch Creek. Residents or facilities that use community water or individual wells within the study area were identified and well records obtained for selected wells based on their spatial distribution. This information was used to determine the aquifer residents or facilities utilized. Accessible well records provided a description of well construction, well depth, and sediment composition at different depths. This data was critical to the overall project objective, because the descriptions of depths and lithology could be correlated to one of the three aquifers, based on their known properties. In addition, well casing type had to be identified because of the potential impact of water contamination by Fe. Study sites that had individual wells were selected and plotted throughout sectors of the study area in order to provide the best spatial coverage within the drainage basin. Individual well samples were taken at study sites located

along Futch Creek Road, Bald Eagle Lane, and Creekside Lane, all which were within the drainage system that was determined to supply the Futch Creek springs. In addition, at each site, both a shallow well finished in the Castle Hayne Limestone aquifer and a deep well finished in the Peedee Sandstone aquifer were selected for comparative studies.

Four springs in the south branch of Futch Creek were selected and marked with a stake. The spatial distribution of these springs covered the entire length of the creek, in order to examine potential differences between upper branch and lower branch sectors. In addition, Plantation Village and the Cornelia Nixon Nursing Home were also added to the study in order to characterize the groundwater drainage more inland and up-gradient of Futch Creek. Samples were collected once a month on a falling tide, on the same day, for a full year (February 2001-January 2002).

Water Collection

The four Futch Creek springs were sampled monthly for one year, during periods of low tide. Sampling was done at low tide because of enhanced accessibility and the decreased potential of surface water contamination. All springs discharged freshwater through large sinkhole-like depressions in the surface. Samples were taken using a 1 L polycarbonate horizontal water-sampling bottle. The bottle was lowered into the sinkholes as far down as possible without reaching the bottom and without disturbing any sediment within the hole. This provided the best possible sample without surface water and sediment contamination. Once the samples were taken, a portion was poured into a 500 mL polyethylene bottle, after it was rinsed three times with the sample, and stored for NO_3^-, Cl^-, SO_4^{2-}, and TRP analysis. A portion of the sample was poured into two 20 mL polyethylene bottles containing 800 µL of phenol solution in order to preserve the sample for NH_4^+ analysis (Parsons et al., 1984). A 50 mL polypropylene syringe and 0.45 µm, 25 mm diameter cellulose acetate filters were used to filter 50 mL of each sample in order to remove particles for the dissolved Fe analysis. Each 50 mL sample was poured into two 20 mL polyethylene bottles that had been rinsed three times with the filtered sample. All samples were put on ice for preservation during the collection period.

Well samples were taken either from the exterior, untreated or unfiltered faucets, of private homes or directly from the well at on-site well houses. In all cases, the faucets were left running for several minutes until the pumps had turned on, in order to avoid collection of stagnant samples and to ensure a better representative sample of well water. A 500 mL polyethylene bottle and four 20 mL polyethylene bottles were filled with well water under the same conditions as the spring water samples and placed on ice.

Well Cutting Collection

Well cuttings were collected from two wells in the study area that were being drilled by local water well companies during the study period. These wells provided representative material from the different aquifers. Samples were taken every 2-3 m with a shovel directly from the outflowing mudstream while the well was being drilled. Once the water had been decanted from the sample, the sediment was placed in a plastic bag and labeled with the site location and the depth from which it was taken. The samples were taken to the laboratory, where they were wet-sieved through a US Standard 230 mesh sieve, with the sample remaining on the screen collected. This removed most of the organic and clay and silt size particles (<2 to 62 µm). After sieving, samples were washed and dried under a heat lamp for ~45 min. They were cooled and placed in labeled bags. Samples were examined under a binocular microscope for composition, grain size and sorting. Sediments examined ranged from sand size to gravel size (62 µm to >2 mm).

One of the wells was located at Cornelia Nixon Nursing home, which is located up-gradient from Futch Creek and nearby golf courses (Fig.1). This well was 43 m deep; however, no samples were available for the upper 21 m. Well cuttings collected provided information from

the Castle Hayne Limestone through to the upper part of the Peedee Formation.

The other well was located on Bald Eagle Lane, along the Intracoastal Waterway, downgradient from Futch Creek and nearby golf courses (Fig. 1). This well was drilled to a depth of 18 m and provided information from the surface into the upper part of the Castle Hayne Limestone.

LABORATORY ANALYSIS

All water samples, except those used for Fe and NH_4^+ analysis, were returned to the laboratory and immediately frozen at -10° C for preservation until future analysis. Samples collected for NH_4^+ analysis were refrigerated at ~2° C. Samples for Fe analysis were preserved by acidification with 50 µL of 6 M trace metal grade HCl.

Nitrate, Sulfate, and Chloride

Nitrate, SO_4^{2-}, and Cl^- were analyzed using a Dionex QIC -Z ion chromatograph after samples were brought to room temperature. Mixed standard solutions containing 10 to 61 µM NO_3, 126 to 759 µM SO_4^{2-}, and 494 to 3949 µM Cl^- were analyzed, and the resulting standard curves used to quantify analyte concentrations in the samples.

Ammonium

Ammonium analysis was completed within a week after collection. Using the 20 mL samples that contained the phenol solution, analysis was done using the experimental procedures described by Parsons et al. (1984) for the spectrophotometric determination of NH_4^+. Sample absorbances were read at 640 nm using a 1-cm cell on a Cary 100 spectrophotometer. Five mixed standard solutions containing 0 to 92.90 µM NH_4^+ were analyzed, and the resulting standard curve used to quantify NH_4^+ concentrations in the samples.

Iron

Experimental procedures for total dissolved Fe were modified from the ferrozine method described by Stookey (1970). Sample absorbances were read at 562.2 nm using a 1-cm cell on the Cary 100 spectrophotometer. Six mixed standard solutions containing 0.00 to 9.89 µM Fe were analyzed, and the resulting standard curve used to quantify total dissolved Fe concentrations in the samples.

Phosphate

Total reactive PO_4^{3-} (TRP) analysis was conducted using the 500 mL samples that were brought to room temperature. Experimental procedures were described by Parsons et al. (1984) for determination of total reactive PO_4^3. Sample absorbances were read at 885 nm using a 10-cm cell on the Cary 100 spectrophotometer. Five mixed standard solutions containing 0.00 to 4.02 µM PO_4^{3-} were analyzed, and the resulting standard curve used to quantify total reactive phosphate concentrations in the samples.

Data processing and formatting was done using Microsoft Excel™ and the Cary 100 software, which created standard curves for every run and converted all absorbency and peak area readings to concentrations.

RESULTS

Nutrient and dissolved Fe concentrations not only varied between the two aquifers studied, but also within each aquifer depending upon well location and the time of year. Nutrient concentrations were measured from February 2001 to January 2002. Dissolved Fe concentrations were only measured from June 2001 to January 2002.

Peedee Sandstone Aquifer

Nitrate concentrations in the Peedee sandstone aquifer were extremely low, ranging from non-detectable to 0.7 mg/L, with an average concentration less than 0.1 mg/L (Roberts,

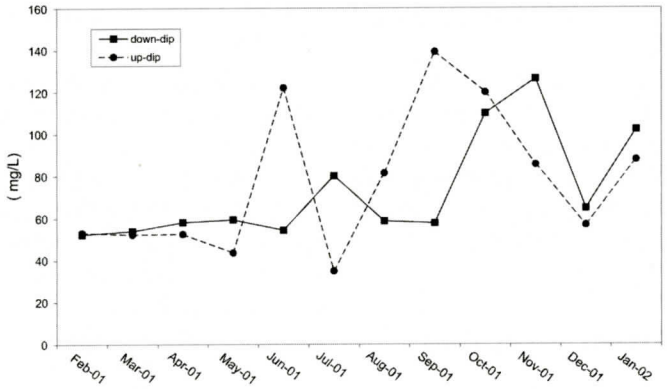

Figure 4. Average ammonium concentrations from February 2001-January 2002 in wells finished in the up-dip and downdip in the Peedee sandstone aquifer.

2002). EPA and North Carolina State Standards for NO_3^- expressed as N are 10 mg/L (North Carolina Administrative Code, 1998). No seasonal trends or differences were seen between wells located up-dip or down-dip within the drainage basin of the study area for this aquifer.

Sulfate concentrations in the Peedee sandstone aquifer were also very low, ranging from non-detectable to 10.6 mg/L with an average concentration of 1.5 mg/L (Roberts, 2002). The North Carolina State Standard for this constituent is 250 mg/L (North Carolina Administrative Code, 1998). Similarly, no seasonal trends or differences were seen between wells located up-dip or down-dip within the drainage basin of the study area for this aquifer.

Chloride concentrations in the Peedee sandstone aquifer ranged from 55 to 240 mg/L, with an average concentration of 89 mg/L (Roberts, 2002). EPA and North Carolina State Standards for Cl^- are 250 mg/L (North Carolina Administrative Code, 1998). Chloride concentrations tended to increase slightly for most well sites in July of 2001 and January of 2002. The maximum concentration of 240 mg/L at site PN-E occurred in March 2001 and did not correlate with Cl^- concentrations at other sites. A slight decrease in Cl^- concentrations was seen during late summer-early fall of 2001 for all well sites. The wells located down-dip in the drainage basin tended to have slightly higher Cl^- concentrations overall than those wells located up-dip in the drainage basin. That is, Peedee wells with higher Cl^- concentration are nearer to the Atlantic Intracoastal Waterway.

Ammonium concentrations in the Peedee sandstone aquifer varied from non-detectable to 240 µg/L, with an average concentration of 76 µg/L (Roberts, 2002). There is no state standard for this constituent. Ammonium concentrations for each site in the study area generally followed the same pattern throughout the study period. Increased concentrations were typically seen in the late spring and later summer-early fall of 2001, with the maximum concentration of 240 µg/L found at site PN-E in July. Decreased concentrations were mainly seen in the winter. Ammonium concentrations were generally consistent among wells within the drainage basin of the Peedee sandstone aquifer during any one season; however, seasonal fluctuations in average NH_4^+ concentration for the up-dip sites slightly lagged behind those of the down-dip sites (Fig. 4)

Dissolved Fe concentrations for the Peedee sandstone aquifer showed a slight difference in concentration between up-dip and down-dip locations of the drainage basin (Fig. 5a and 5b). Up-dip concentrations varied from non-detectable to 2.5 mg/L, with an average concentration of 0.4 mg/L (Fig. 5a). The North Carolina State Standard for dissolved Fe is 0.3 mg/L (North Carolina Administrative Code, 1998). Increased concentrations were generally seen in September of 2001, with the maximum concentration of 2.5 mg/L at site PN-J. Decreased concentrations were generally seen in November of 2001. Down-dip concentrations for the Peedee

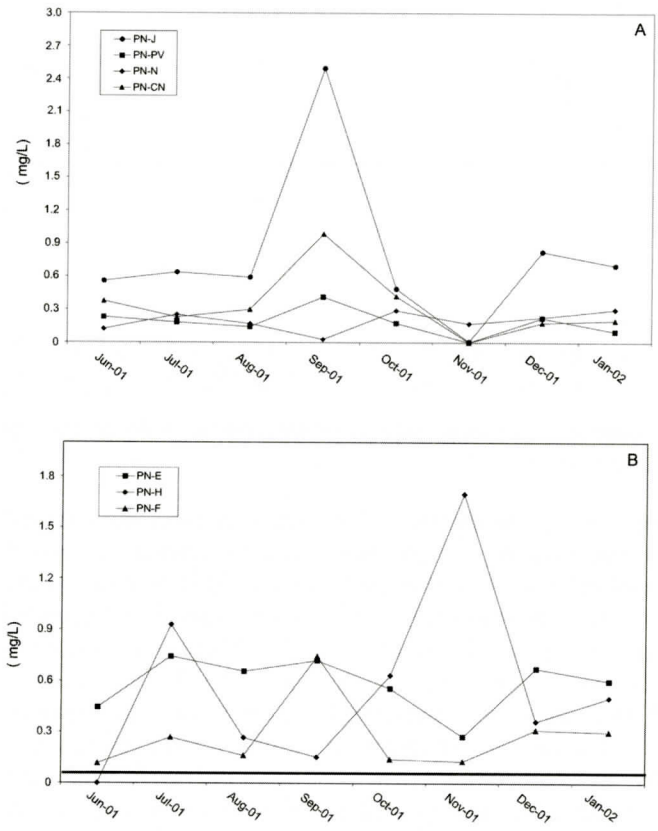

Figure 5. a) Fe concentrations from June 2001 to January 2002 in wells finished in the up-dip Peedee sandstone aquifer; b) Fe concentrations from June 2001 to January 2002 in wells finished in the downdip Peedee sandstone aquifer.

sandstone aquifer varied from 0.0 to 1.7 mg/L, with an average concentration of 0.5 mg/L (Fig. 5b). All dissolved Fe concentrations increased in July and most in December of 2001 for most down-dip sites. However, between July and December concentrations fluctuated monthly with little correspondence to one another, except in August 2001 when all sites had a slight decrease in concentration. The maximum concentration of 1.7 mg/L occurred in November at site PN-H.

Only low concentrations of TRP were found in samples from the Peedee sandstone aquifer. Phosphate was expressed as P and ranged from non-detectable to 0.04 mg/L, with an average concentration of 0.01 mg/L (Roberts, 2002). There is no state standard for this constituent. No trends or differences were seen between wells located up-dip or down-dip within the drainage basin of the study area for this aquifer, hence TRP concentrations are not illustrated.

Castle Hayne Limestone Aquifer

Sulfate concentrations for the Castle Hayne Limestone aquifer were slightly higher than those for the Peedee sandstone aquifer. Concentrations for the Castle Hayne Limestone aquifer ranged from non-detectable to 75 mg/L, with an average concentration of 16 mg/L (Roberts, 2002). Little difference was seen between up-dip and down-dip locations in the drainage basin of the Castle Hayne Limestone aquifer, in comparison to one another and individually throughout the study period. Nitrate concentrations in the Castle Hayne Limestone aquifer

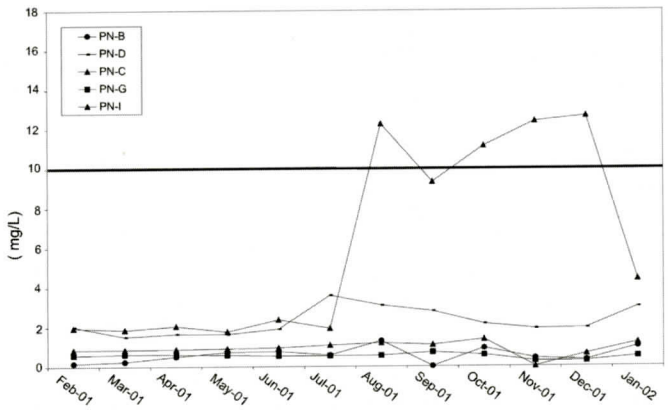

Figure 6. Nitrate concentrations from February 2001-January 2002 in wells finished in the down-dip Castle Hayne Limestone aquifer.

showed differences between up-dip and down-dip locations in the drainage basin throughout the study period, and in some cases, were much higher than the NO_3^- concentrations of the Peedee sandstone aquifer. Up-dip concentrations in the Castle Hayne Limestone aquifer were fairly small and ranged from non-detectable to 1.7 mg/L, with an average concentration of 0.4 mg/L. There were no significant trends or patterns seen in the up-dip values throughout the study period. Many of the down-dip NO_3^- concentrations in the limestone aquifer were significantly higher. The range in this aquifer was from non-detectable to 12.6 mg/L, with an average concentration of 2.1 mg/L (Fig. 6). Concentrations slightly increased in the late summer and early fall for most down-dip sites; however, overall concentrations remained fairly constant for this time interval. Site PN-C was the highest overall, having concentrations above or close to the state standard from August 2001 to December 2001, with a maximum concentration of 12.6 mg/L in December. In the early winter, most down-dip sites decreased in NO_3 concentrations, and then increased again slightly in January 2002, except for site PN-C, which decreased greatly in January.

Chloride concentrations for the Castle Hayne Limestone aquifer were slightly higher than those for the Peedee sandstone aquifer. Concentrations for the Castle Hayne Limestone aquifer ranged from 8.3 to 344 mg/L, with an average concentration of 95 mg/L (Roberts, 2002). Chloride concentrations in this aquifer were relatively constant throughout the study period; however, decreased concentrations were seen from October to December of 2001 for most sites. Little to no variance was seen between up-dip and down- dip locations within the drainage basin of the Castle Hayne Limestone aquifer, except for site PN-G, which was located in the down-dip region. This site was the highest overall, having concentrations above or near the state standard for the duration of the study period. The maximum concentration of this site was 344 mg/L in February 2001.

Ammonium concentrations in the Castle Hayne Limestone aquifer were similar to those of the Peedee sandstone aquifer only in the up-dip location of the drainage basin. Up-dip NH_4^+ concentrations for the Castle Hayne Limestone aquifer ranged from non-detectable to 226 µg/L, with an average concentration of 36 µg/L (Fig. 7). Higher NH_4^+ concentrations occurred in the late summer to early fall, with a slight increase occurring in January 2002. However, overall concentrations were generally low in the winter. Ammonium concentrations were very low in the down-dip wells of the Castle Hayne Limestone aquifer for the duration of the study period, ranging from non-detectable to 15.1 µg/L and averaging 1.1 µg/L (Roberts, 2002).

Dissolved Fe concentrations for the Castle Hayne Limestone aquifer were lower overall than the Peedee sandstone aquifer concentrations, except for site PN-O. Concentrations

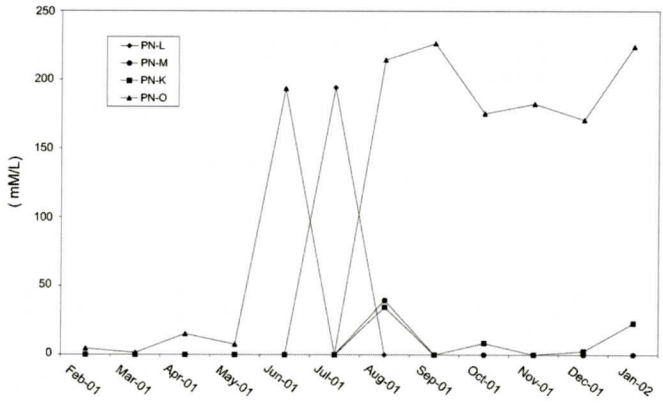

Figure 7. Ammonium concentrations February 2001-January 2002 in wells finished in the up-dip Castle Hayne Limestone aquifer.

ranged from non-detectable to 7.0 mg/L, with an average concentration of 0.6 mg/L (Roberts, 2002). Very minor increases in concentrations occurred in July, September and December of 2001 for most up-dip sites. Little to no variation was seen between up-dip and down-dip locations within the drainage basin of the Castle Hayne Limestone aquifer (Fig. 8a and Fig. 8b),

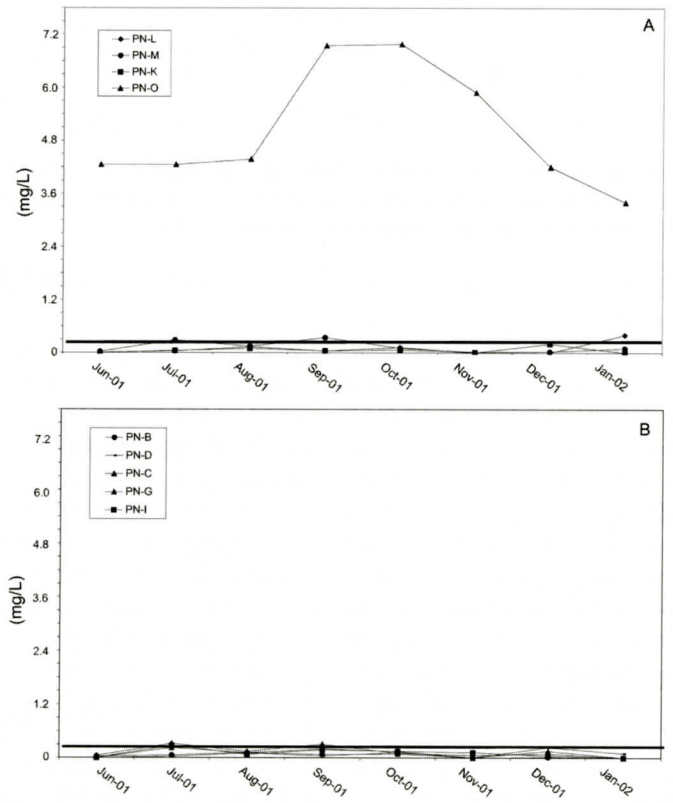

Figure 8. a) Fe concentrations from June 2001-January 2002 in wells finished in the up-dip Castle Hayne Limestone aquifer; b) Fe concentrations from June 2001-January 2002 in wells finished in the downdip Castle Hayne Limestone aquifer.

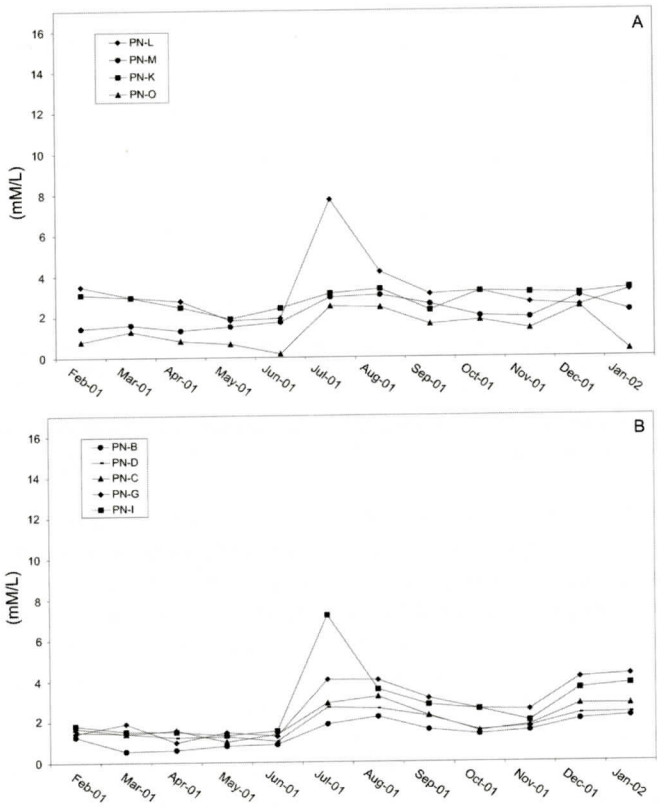

9.a) Phosphate concentrations from February 2001-January 2002 in wells finished in the up-dip Castle Hayne Limestone aquifer; b) Phosphate concentrations from February 2001-January 2002 in wells finished in the downdip Castle Hayne Limestone aquifer.

except for site PN-O, which was located in the up-dip region. Concentrations for PN-O were above the state standard for the entire study period, ranging from 3.4 to 7.0 mg/L, with the maximum concentration occurring in October 2001. Dissolved Fe concentrations for all sites other than PN-O tended to decrease in August and October of 2001.

Total reactive PO_4^{3-} concentrations for the Castle Hayne Limestone aquifer were higher than those of the Peedee sandstone aquifer. Phosphate was expressed as P and ranged from 0.01 to 0.24 mg/L, averaging at 0.07 mg/L (Fig. 9a and Fig. 9b). Although concentrations for this constituent seemed to fluctuate just slightly throughout the study period, small increases were seen in July of 2001 for all sites.

Futch Creek Springs

The quality of spring samples was dependent upon the extremity of the low tides and the location of the spring sampled. Springs FC-S3 and FC-S4 provided the most representative samples of spring water due to their location in the upper south branch of Futch Creek (Fig.1). Nitrate concentrations for the springs were sympathetic with those of the Castle Hayne Limestone aquifer. Concentrations ranged from non-detectable to 15.9 mg/L, with an average concentration of 1.4 mg/L (Fig. 10). A minor increase in concentrations could be observed in the late summer to early fall. Spring FC-S1 had the highest values during this period and into the early winter months, with the maximum concentration of 15.9 mg/L, occurring in December 2001.

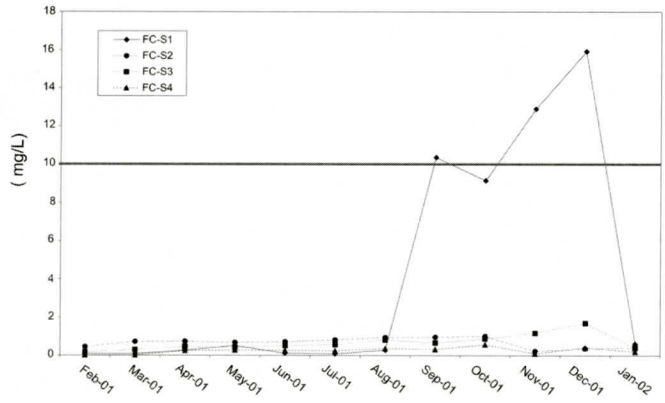

Figure 10. Nitrate concentrations from February 2001-January 2002 in four Futch Creek springs.

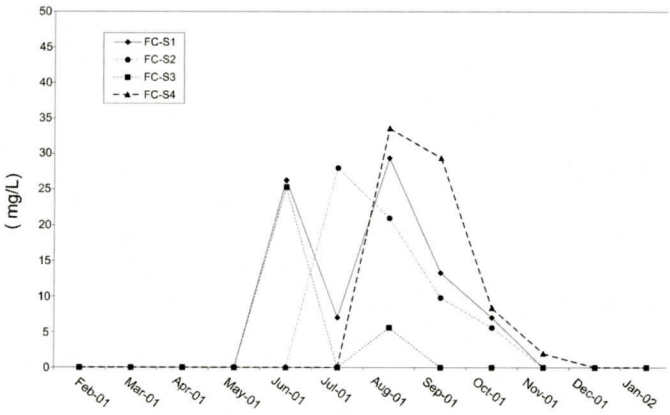

Figure 11. Ammonium concentrations from February 2001-January 2002 in four Futch Creek springs.

Sulfate concentrations for all springs ranged from 29 to 1610 mg/L, with an average concentration of 290 mg/L (Roberts, 2002). Fluctuations did occur throughout the study period for this parameter for all springs, with no particular trends or patterns.

FC-S3 and FC-S4 provided the best representative samples for Cl^- analysis. Chloride concentrations for all springs ranged from 77 to 11,100 mg/L, with an average concentration of 1818 mg/L (Roberts, 2002). Similarly, seasonal fluctuations did occur throughout the study period for this parameter for all springs, however with no particular trends or patterns.

Ammonium concentrations for the springs resembled the NH_4^+ values for the down-dip wells of the Castle Hayne Limestone aquifer. Concentrations for the springs ranged from non- detectable to 34 µg/L, with an average concentration of 5.2 µg/L (Fig. 11). Increased concentrations were seen in the summer and early fall.

Dissolved Fe concentrations for the springs were not similar to the concentrations of the Peedee sandstone aquifer and most of the Castle Hayne Limestone aquifer; however, site PN-O of the upper Castle Hayne displayed similar seasonal patterns to the springs (Roberts, 2002). Concentrations for the springs ranged from 0.0 to 2.8 mg/L, with an average concentration of 0.8 mg/L (Fig. 12). Increased concentrations were observed in the late summer and early fall. Concentrations decreased greatly in the late fall and winter months.

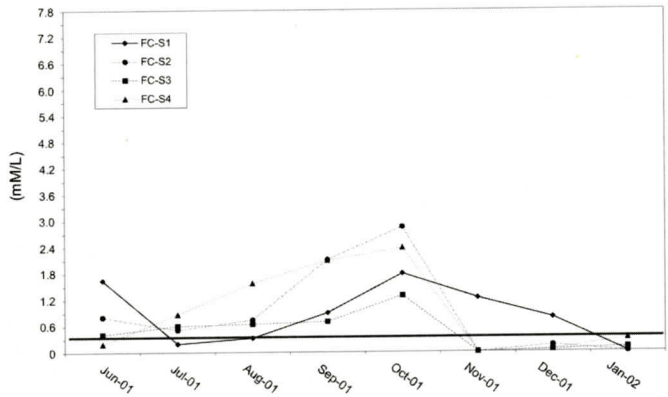

Figure 12. Fe concentrations from June 2001-January 2002 in four Futch Creek springs.

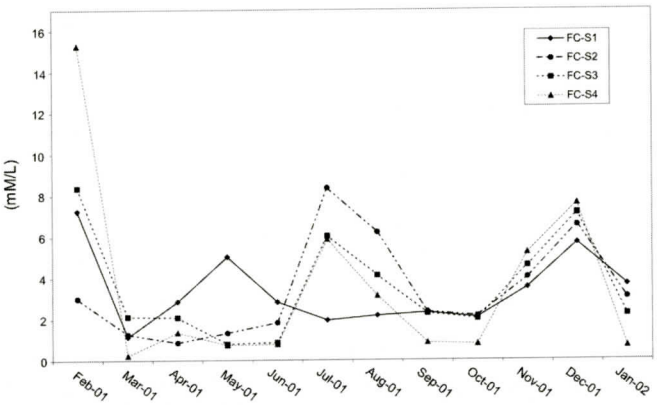

Figure 13. Phosphate concentrations from February 2001-January 2002 in four Futch Creek springs.

Total reactive PO_4^{3-} concentrations for the springs resembled the Castle Hayne Limestone aquifer TRP values. Concentrations for the springs were expressed as P and ranged from 0.01 to 0.47 mg/L, with an average concentration of 0.11 mg/L (Fig. 13). The highest concentrations were seen in February, July and December of 2001. Decreased values were seen in early summer and late fall.

DISCUSSION AND CONCLUSIONS

The nature and composition of chemical constituents in the Peedee sandstone aquifer do not resemble those in the Castle Hayne Limestone aquifer (Table 1). These differences relate to lithology, depth differences, subsurface stratigraphy, hydraulic conductivity, geological heterogeneity, and source of recharge. The Peedee Sandstone aquifer is the deepest freshwater-bearing aquifer in New Hanover County. In the western part of the county, along the Northeast Cape Fear River, it occurs near the surface and receives direct infiltration of surface water. In the eastern part of the county, the Peedee Sandstone aquifer occurs at a depth of greater than 30 m below sea level, and is overlain by a thick sandy clay aquiclude (Fig. 3). Therefore, direct surface activity in the Porters Neck area probably does not have a short-term effect on the Peedee Sandstone aquifer. The Castle Hayne Limestone aquifer, however, is shallower and may have direct connection to the surface in the Porters Neck area. Thus, it re-

Table 1. Average nutrient and Fe concentrations for Futch Creek springs and the Castle Hayne and Peedee sandstone aquifers, Porters Neck area, New Hanover County, North Carolina.

	NO_3 (mg/L)	SO_4 (mg/L)	Cl (mg/L)	NH_4 (µg /L)	Fe (µg/L)	PO_4 (µM/L)
Castle Hayne						
Updip	0.4	9.9	68.9	35.8	1.3	2.4
Downdip	2.1	20.6	116.3	1.1	0.1	2.1
Peedee						
Updip	0.0	1.2	66.7	77.4	0.4	0.4
Downdip	0.0	1.8	118.1	73.2	0.5	0.2
Springs	1.4	289.9	1818.4	5.2	0.8	3.5

ceives its recharge on-site, through the direct percolation of water from the surface through to the underlying sediment. The Castle Hayne Limestone aquifer in this area may also receive water by lateral flux from areas west of U.S. Highway 17 (Lautier, 1994). In some cases, the Castle Hayne Limestone aquifer can exist as the water table aquifer, where no confining unit occurs in the surficial sediments, therefore exposing the limestone. Hence, in the Porters Neck Area, the Peedee sandstone aquifer is less affected by any surface activity, whereas the Castle Hayne Limestone aquifer is susceptible to natural and anthropogenic surface activities.

Nitrogen Speciation

Nitrogen species are derived from plants, agricultural activities, septic systems, and fertilizers (Drever, 1997). Its speciation is dependent upon the available oxygen in an environment, or whether conditions are aerobic or anaerobic. In aerobic environments, where oxygen is available, nitrogen exists as nitrate (NO_3^-). In anaerobic environments, where oxygen is depleted, nitrogen exists as ammonium (NH_4^+). Temperature variances affect the amount of oxygen that is supplied to the various environments. Normally, in the colder fall and winter months more oxygen is available to the groundwater system, and in the warmer spring and summer months less oxygen is available to the system. This is dictated by the intensity of microbial processes and the degradation of organic matter. During times of increased temperatures, there is more bio-productivity and thus, more degradation of organic matter. Therefore, an increase in the utilization of oxygen by bacteria occurs and less oxygen is available to the groundwater system (Petry, et al., 2002). During times of decreased temperatures, the inverse of this relationship is seen.

As stated earlier, the North Carolina State Standard for NO_3^- expressed as N is 10 mg/L (North Carolina Administrative Code, 1998). Bain (1970) indicates that NO_3^- concentrations in excess of 3 mg/L generally suggests that a polluting source is nearby such as sewage systems, fertilizers or polluted surface waters.

Overall, the NH_4^+ concentrations in the Peedee sandstone aquifer were higher than the Castle Hayne Limestone aquifer and springs, whereas NO_3^- concentrations in the Peedee sandstone aquifer were lower than the Castle Hayne Limestone aquifer and springs. This is probably due to the highly anaerobic nature of the Peedee sandstone aquifer compared to the more shallow Castle Hayne groundwater system. As the Peedee sandstone aquifer is at such a greater depth than the Castle Hayne Limestone aquifer and springs, the NO_3^- and NH_4^+ concentrations are little affected by surface activity and seasonal variability.

Ammonium concentrations in the up-dip section of the drainage basin for the Castle Hayne Limestone aquifer were fairly high and displayed seasonal variation, whereas the down-dip section had very low concentrations and little seasonal variability. Although overall concentrations were fairly low, higher concentrations were seen in the late summer and early fall. Nitrate levels in the down-dip Castle Hayne Limestone aquifer showed the highest concentrations and displayed seasonal

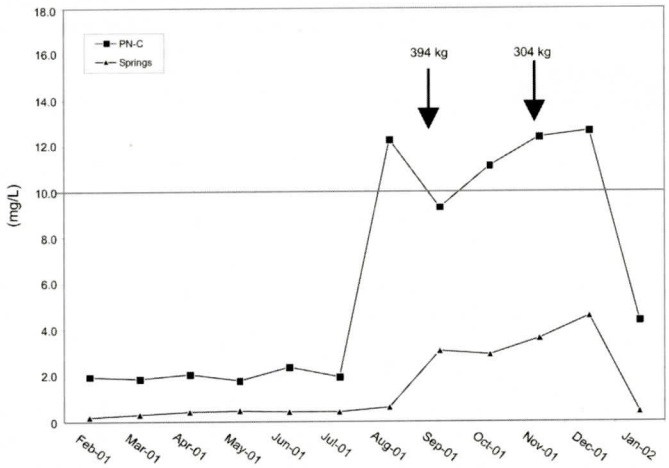

Figure 14. Average major fertilization periods for three New Hanover County golf courses in 1982 (Mallin et al., 2002) compared to nitrate concentrations expressed as N (mg/L) for site PN-C from the downdip Castle Hayne Limestone aquifer and for the average of the four Futch Creek springs, February 2001 through January 2002.

trends throughout the study period (Fig. 6). However, in the late summer and early fall, when concentrations should have been lower due to increased temperatures, NO_3^- concentrations were actually higher. This contradiction suggests that an external source, such as fertilizer, had an effect on the amounts of NO_3^- in these systems. Nitrate concentrations also varied within the down-dip section of the drainage basin for the Castle Hayne Limestone aquifer. Down-dip Castle Hayne sites located along Bald Eagle Lane had the highest NO_3^- concentrations. This variation could be due to the location of the sites within the down-dip section of the drainage basin, the subsurface topography, and the various flow paths of the groundwater system.

Ammonium concentrations in the springs resembled those of the down-dip Castle Hayne Limestone aquifer sites, with apparent seasonal variability. Similarly, overall concentrations were fairly low; however, higher concentrations were seen in the late summer and early fall. Seasonal variability for NO_3^- concentrations in the springs resembled those observed at the down-dip Castle Hayne Limestone aquifer sites. Although NO_3^- concentrations in the springs generally were not as elevated as the down-dip Castle Hayne Limestone aquifer sites, they were still significantly higher than values from the Peedee sandstone aquifer, and presumably could be responsible for algae blooms that occur at certain times of the year (Mallin et al., 1996).

Mallin et al. (1996) suggested that the source for NO_3^- in a spring located in the upper south branch of Futch Creek could be from a septic field drainage area. Bain (1970) suggested that nitrogen fertilizers probably contaminated a well located in Wilmington, NC, along the Northeast Cape Fear River. The Porters Neck Golf Course is located in the up-dip part of the drainage basin in the study area. Figure 14 compares times of major fertilization of three New Hanover County golf courses in 1982, with the average NO_3^- concentrations in Futch Creek springs and down dip wells finished in the Castle Hayne Limestone aquifer. These data suggest that the Porters Neck Golf Course might be a potential source for NO_3^- in the Castle Hayne in some areas that are located down-dip from the golf course within the drainage basin.

Sulfate and Chloride

Sulfur-bearing minerals such as pyrite, mar-

casite are present in the underlying sediments of New Hanover County, and these minerals, as well as the calcium and magnesium sulfates frequently associated with shell and limestone beds are soluble in groundwater systems (Bain, 1970). Sulfur can also be found by its reduction in the presence of organic material and bacteria; a process more commonly observed in the Peedee sandstone aquifer. Sulfate can also be introduced to the system via the intrusion of brackish waters, a process more commonly seen in some areas of the Castle Hayne Limestone aquifer. Chloride is incorporated into the system by brackish water or saltwater intrusion. The rate of flushing of the New Hanover County aquifers by freshwater is dependent upon time, hydraulic head, and the composition of the flushing waters (Bain, 1970) and by water usage.

High Cl^- and SO_4^{2-} concentrations can occur with an increase in water usage and with the intrusion of saltwater or brackish water. However, in order for saltwater intrusion to be considered a factor, concentrations for Cl^- and SO_4^{2-} would have to fluctuate in correspondence with one another in an approximately constant ratio of 19.3, which is the molar ratio of these ions in seawater (Drever, 1997).

Sulfate and Cl^- concentrations were lower in the Peedee sandstone aquifer than in the Castle Hayne Limestone aquifer. The highest concentrations were seen in sites located in the down-dip section of the Peedee sandstone aquifer. Overall, higher Cl^- and SO_4^{2-} concentrations were seen from summer to early winter, probably due to the increased amount of water being used by well owners (Harris, 1998). Fluctuations of these constituents for each site did not occur at a constant ratio; however, when Cl^- concentrations increased or decreased, SO_4^{2-} concentrations reacted in the same manner. The Cl^- to SO_4^{2-} ratio can be altered by the addition or subtraction of SO_4^{2-}. During times of increased oxygen availability, increased oxidation of sulfide minerals would result in increased SO_4^{2-} concentrations, and during times of decreased oxygen availability this process would be diminished, resulting in reduced SO_4^{2-} concentrations. Sulfate can also be taken away from the system by microbial SO_4^{2-} reduction.

Sulfate and Cl^- concentrations in the Castle Hayne Limestone aquifer, like the Peedee sandstone aquifer, were highest at sites located in the down-dip section of the aquifer for the study area. Seasonal variability of Cl^- and SO_4^{2-} in the Castle Hayne Limestone aquifer also resembled the seasonal variability in the Peedee sandstone aquifer, probably for the same reasons as discussed previously. Bain (1970) noticed higher Cl^- and SO_4^{2-} content in the Castle Hayne Limestone aquifer in areas along estuaries and sounds, probably due to saltwater intrusion.

No particular trends or patterns were observed in Cl^- and SO_4^{2-} concentrations for the springs, even for sites FC-S3 and FC-S4. This was probably due to the ease of its contamination by the surface water of Futch Creek during sample collection.

Total Dissolved Iron

Iron is a major component of limestones and sandstones (Drever, 1997). The primary sources of Fe in the hydrosphere are the iron-rich minerals of igneous and metamorphic rocks. Mobilization and redistribution of Fe occurs during chemical weathering of these minerals (Langmuir, 1997). The mobilization of Fe is primarily as the dissolved form Fe^{2+} or as the particulate form $Fe(OH)_3$ (Langmuir, 1997). Under reducing conditions when oxygen availability to the system is low, Fe^{2+} is the dominant form. This kind of condition is created during the warmer spring and summer months of a given year. Increased temperatures and high productivity leads to greater rates of remineralization of organic matter. Essentially, after oxygenic respiration, NO_3^-, Fe and Mn reduction become the more important respiration pathway (Robins, 2002). When oxygen availability to the system increases and temperatures decrease, $Fe(OH)_3$ becomes the dominant form. The same relationship can be seen in sedimentary rocks and soils, as well.

Bain (1970) stated that dissolved Fe concentrations in the Castle Hayne Limestone aquifer ranged between 0.3 and 4.0 mg/L, and that dis-

solved Fe concentrations in the Peedee sandstone aquifer were less than 0.3 mg/L. The Fe concentrations for this study were not consistent with these two values.

Dissolved Fe concentrations for the Peedee sandstone aquifer were higher than the Castle Hayne Limestone aquifer, and were much higher than what Bain (1970) reported. Higher concentrations were seen in the summer and lower concentrations were seen in the winter; however, concentrations were still unusually high for this unit. This is probably because the Peedee Formation is highly anaerobic as opposed to other aquifers, due to its greater depth in the subsurface (Harris, 1998). This particular nature of dissolved Fe in the Peedee sandstone aquifer is localized to the Porters Neck area (Stehman, personal communication, 2002).

In an examination of well cuttings from the Cornelia Nixon Nursing Home well, it is apparent that the Peedee Formation has a high glauconite content, and in some portions there was a significant amount of Fe particulate. There is also a heavy clay content in this unit and some pyrite/marcasite (Harris, 1978). Potential sources for dissolved Fe in the Peedee sandstone aquifer are the dissolution of glauconite and pyrite/marcasite or the dissolution of Fe-rich clays through cation exchange.

The Castle Hayne Limestone aquifer contained the lowest dissolved Fe concentrations for the study area, except for site PN-O. Higher concentrations were seen throughout the study period in this aquifer when temperatures were higher and less oxygen was available to the system. Similarly to the Peedee sandstone aquifer, the dissolved Fe concentrations observed in the Castle Hayne Limestone aquifer were higher than those stated by Bain (1970), supporting the idea that these conditions are probably localized for this unit in this area.

Cuttings from the well along Bald Eagle Lane show the Castle Hayne unit is high in glauconite and that the upper portion of the Castle Hayne has a significant amount of Fe particulates. Dissolved Fe may have been provided to the Castle Hayne Limestone aquifer by the dissolution of glauconite. Site PN-O, which maintained the highest dissolved Fe concentrations for the Castle Hayne Limestone aquifer sites, is located in the upper part of the Castle Hayne; therefore, Fe particulates probably served as a major source of dissolved Fe in the system, along with the dissolution of glauconite.

Dissolved Fe concentrations for the four springs were fairly high. In the summer and early fall concentrations were elevated, since oxygen should have been less available to the system. The high dissolved Fe content probably results from its waters moving through Fe-rich sediments.

Total Reactive Phosphate

The Peedee sandstone aquifer had very small concentrations of TRP throughout the study period. Well cuttings, however, of the Peedee Formation from the Cornelia Nixon Nursing Home indicate that the unit is rich in glauconite and PO_4^{3-} pebbles (see Roberts, 2002). The Castle Hayne Limestone aquifer and the four springs contained the highest amounts of TRP. Well cuttings from the Bald Eagle Lane site indicate that the Castle Hayne is also rich in glauconite and PO_4^{3-} (see Roberts, 2002). The highest concentrations of TRP were seen in the summer and late fall for the Castle Hayne Limestone aquifer and for the springs. Phosphate naturally occurs in the groundwater systems through the dissolution of various minerals and conglomerates, such as glauconite, apatite, or phosphate pebbles, in highly anaerobic environments (Carlyle et al., 2001). Phosphate can also be added to the system by the infiltration of PO_4^{3-} fertilizers from the surface through polluted waters (Bain, 1970). Oxygen availability has an impact on PO_4^{3-} levels in groundwater through its relationship with Fe. During times of high oxygen availability, PO_4^{3-} tends to attach to particulate $Fe(OH)_3$. Usually during periods of warmer temperatures and increased rates of organic matter remineralization, oxygen levels decrease, $Fe(OH)_3$ is reduced to dissolved Fe^{2+}, and PO_4^{3-} is then released into the groundwater as a dissolved ion (Carlyle et al., 2001). Therefore, when dissolved Fe concentrations increase, PO_4^{3-} concentrations should increase, as well.

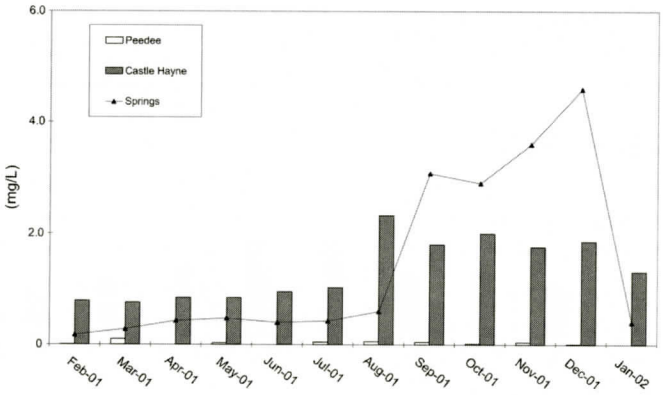

Figure 15. A comparison of nitrate concentrations from February 2001 and January 2002 in Futch Creeks springs, the Peedee sandstone aquifer and the Castle Hayne Limestone aquifer.

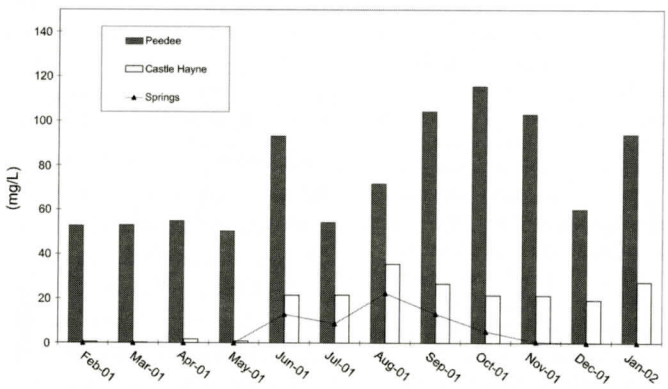

Figure 16. A comparison of ammonium concentrations from February 2001 and January 2002 in Futch Creeks springs, the Peedee sandstone aquifer and the Castle Hayne Limestone aquifer.

When higher dissolved Fe concentrations were seen in these systems, higher TRP concentrations were seen, as well. The Peedee sandstone aquifer is highly anaerobic, contains significant amounts of glauconite and PO_4^{3-} pebbles, but low amounts of TRP. These observations suggest that the dissolution of these minerals has little influence on TRP concentrations in the groundwater. Taking this information into consideration, along with the fact that the Castle Hayne Limestone aquifer and the springs are actually more aerobic than the Peedee sandstone aquifer, suggests that the high TRP concentrations observed in the Castle Hayne Limestone aquifer and springs probably result from an outside source, such as PO_4^{3-} fertilizers from the nearby golf course.

Relationship of Aquifers to Springs

Information provided by NO_3^-, NH_4^+, Fe, and TRP concentrations and seasonal fluctuations for groundwater systems involved in this study suggest that the four springs originate from the Castle Hayne Limestone aquifer. Figures 15, 16, 17, and 18 compare the average concentrations and seasonal trends of these constituents for the Castle Hayne and Peedee sandstone aquifers to the average concentrations and seasonal trends of the springs.

SUMMARY

The concentrations of NO_3^-, Cl^-, SO_4^{2-}, NH_4^+, TRP and dissolved Fe in the Peedee and Castle Hayne Limestone aquifers vary between

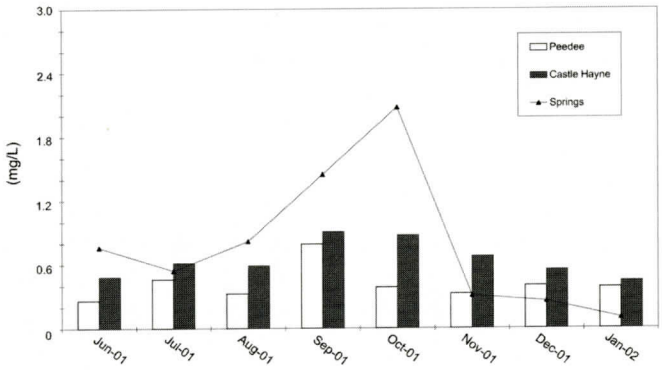

Figure 17. A comparison of iron concentrations from June 2001 and January 2002 in Futch Creek springs, the Peedee sandstone aquifer and the Castle Hayne Limestone aquifer.

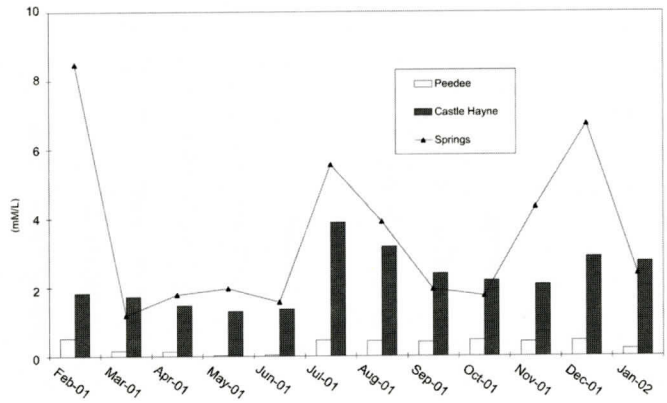

Figure 18. A comparison of phosphate concentrations from February 2001 and January 2002 in Futch Creeks springs, the Peedee sandstone aquifer and the Castle Hayne Limestone aquifer.

each other and seasonally. The major points of the study are summarized below.

- The Peedee sandstone aquifer in the Porters Neck area of New Hanover County is well protected from any surface activity because of its depth and the location of its recharge area to the west.
- Nitrate, Cl^-, SO_4^{2-} and TRP levels are significantly lower in the Peedee sandstone aquifer when compared to state standards.
- Ammonium concentrations are elevated in the Peedee sandstone aquifer twice within the study period due to the highly anaerobic nature of this aquifer.
- Dissolved Fe concentrations in the Peedee sandstone aquifer are also influenced by the anaerobic environment, as well. The higher concentrations of this constituent are due to the dissolution of Fe particulates and glauconite. A majority of the Peedee sandstone aquifer sites exceeded North Carolina state standards for iron content.
- The Castle Hayne Limestone aquifer is significantly influenced by surface activity and seasonal variability because of its shallower depth and its on-site recharge. This recharge occurs either from water which has percolated through the overlying surficial sediment, or from direct recharge in areas where the Castle Hayne Limestone aquifer is located at the surface and exists as the water table aquifer.
- Nitrate, NH_4^+, and TRP content is higher in the down-dip section of the Castle Hayne Limestone aquifer for certain sites

possibly due to heavy fertilization occurring at the Porters Neck Golf Course, which is located up-dip in the drainage basin of the study area. In some cases, NO_3^- concentrations in the down-dip area of the drainage basin exceeded North Carolina State Standards.

- Chloride and SO_4^{2-} content in the Castle Hayne Limestone aquifer increased during the warmer months of the study period, when more water was being pumped out of the aquifer, enabling saltwater to intrude and replace discharged freshwater.
- High dissolved Fe content in the Castle Hayne Limestone aquifer was due to the dissolution of Fe particulates and glauconite. The highest concentrations of this constituent occurred during warmer months of the study period, when little oxygen was available to the groundwater system, creating a reduced environment. In some cases, the dissolved Fe content of the Castle Hayne Limestone aquifer exceeded North Carolina State Standards.
- Nutrient and dissolved Fe analyses of the two aquifers and springs located in the south branch of Futch Creek suggest that the springs originate from the Castle Hayne Limestone aquifer.
- Although in most cases the NO_3^- concentrations of these springs did not exceed North Carolina State Standards for drinking water, they can still be considered detrimental to the ecological environment. Algae blooms were seen at certain times of the year during the study period, probably due to elevated NO_3^- and TRP concentrations.

ACKNOWLEDGMENTS

This paper is based on a master's thesis by the senior author completed at the University of North Carolina at Wilmington. The authors thank the Northeast New Hanover Conservancy who provided funding for the project, especially Paul Foster (deceased), and Paul Thayer, Charles Stehman and Stephen Skrabal for their assistance. Thorough reviews by Thomas Scott and Eric Henry are greatly appreciated and significantly improved the paper.

REFERENCES CITED

Bain, L.G., 1970, Ground water resources of New Hanover County, North Carolina, North Carolina Department of Water & Air Resources: Groundwater Bulletin 17, p. 61.

Carlyle, G.C., Hill, A.R., 2001, Groundwater phosphate dynamics in a river riparian zone: Effects of hydrologic flowpaths, lithology, and redox chemistry: Journal of Hydrology, v. 247, p. 151-168.

Dockal, J.A., Harris, W.B., Laws, R.A., 1998, Late Maastrichtian sediments on the north flank of the Cape Fear Arch, North Carolina: Southeastern Geology, v. 37, p. 149-159.

Drever, J.I., 1997, The geochemistry of natural waters: Surface and groundwater environments: Prentice Hall, Inc., Upper Saddle River, New Jersey, 436 p.

Gramling, C.M., 2003, A radiocarbon method and multitracer approach to quantifying groundwater discharge to coastal waters (Ph.D. dissertation): Massachusetts Institute of Technology, 347 p.

Harris, W.B., 1978, Stratigraphic and structural framework of the Rocky Point Member of the Cretaceous Peedee Formation, North Carolina: Southeastern Geology, v.19, p. 207-229.

Harris, W.B., 1998, Ground water monitoring Porters Neck and Figure Eight Island areas, New Hanover County, North Carolina: Final report to Northeast New Hanover Conservancy, 35 p.

Langmuir, D., 1997, Aqueous environmental geochemistry: Prentice Hall, Inc., Upper Saddle River, New Jersey, 596 p.

Lautier, J.C., 1994, Wilmington harbor ground water study interim report, North Carolina Department of Environment, Health, and Natural Resources Division of Water Resources, Raleigh, North Carolina, 69 p.

Lautier, J.C., 1998, Hydrogeologic assessment of the proposed deepening of the Wilmington harbor shipping channel, New Hanover and Brunswick Counties, North Carolina, North Carolina Department of Environment, Health, and Natural Resources Division of Water Resources, Raleigh, North Carolina, 54 p.

LeGrand, Harry E., 1982, New Hanover county aquifer management program, Wilmington, NC, May 1982, 20 p.

Mallin, M.A., Cahoon, L.B., Manock, J.J., Merritt, M.F., Posey, M.H., Sizemore, R.K., Alphin, T.D., Williams, K.E., and Hubertz, E.D., 1996, Water quality in New Hanover County tidal creeks: Futch Creek headwaters investigation: University of North Carolina at Wilmington Center for Marine Science Research Report, 4 p.

Mallin, M.A., Cahoon, L.B., Manock, J.J., Merritt, J.F., Posey, M.H., Sizemore, R.K., Webster, W.D., and Alphin, T.D., 1998a, A four-year environmental analy-

sis of New Hanover County tidal creeks, 1993-1997: University of North Carolina at Wilmington Center for Marine Science Research Report 98-01, 62 p.

Mallin, M.A., Cahoon, L.B., Manock, J.J., Merritt, J.F., Posey, M.H., Alphin, T.D., Parsons, D.C., and Wheeler, T.L., 1998b, Environmental quality of Wilmington and New Hanover County watersheds: Futch Creek: University of North Carolina at Wilmington Center for Marine Science Research Report 98-03, 4p.

Mallin, M.A., Cahoon, L.B., Lowe, R.P., Merritt, J.F., Sizemore, R.K., and Williams, K.E., 2000, Restoration of shellfishing waters in a tidal creek following limited dredging: Journal of Coastal Research, v. 16, p. 40-47.

North Carolina Administrative Code, 1998, Department of Environment and Natural Resources, Title 15A, November 1998, 41 p.

Parsons, T.R., Maita, Y., Lalli, C.M., 1984, A manual of chemical and biological methods for seawater analysis: Oxford, Pergamon, 173 p.

Petry, J., Soulsby, C., Malcolm, I.A., Youngson, A.F., Hydrological controls on nutrient concentrations and fluxes in agricultural catchments: The Science of the Total Environment, Elsevier, in press.

Robins, N.S., Groundwater quality in Scotland: major ion chemistry of the key groundwater bodies: The Science of the Total Environment, Elsevier, in press.

Sohl, N.M, and Owens, J.P, 1992, Cretaceous stratigraphy of the Carolina Coastal Plain; *in* Horton, Jr., J.W. and Zullo, V.A. (eds.), The geology of the Carolinas: Knoxville, University of Tennessee Press, p. 191-220.

Soil Survey of New Hanover County, North Carolina, 1977, United States Department of Agriculture Soil Conservation Service, 69 p.

Stookey, L.L., 1970, Ferrozine: a new spectrophotometric reagent for iron: Analytical Chemistry, v. 42, p. 779-781.

SOUTHEASTERN GEOLOGY
V. 43, No. 2, November 2004, p. 103-111

AQUEOUS CARBONATE GEOCHEMISTRY OF THE UPPER FLORIDAN AQUIFER BELOW THE DOUGHERTY PLAIN, GEORGIA: EFFECTS OF SEMI-CONFINING CONDITIONS

SETH ROSE

Department of Geology
Georgia State University
P.O. Box 4105
Atlanta, GA 30302-4105
e-mail: geoser@panther.gsu.edu

ABSTRACT

The aqueous carbonate geochemistry of the Upper Floridan aquifer (UFA) below the Dougherty Plain of southwestern Georgia was analyzed using data from 55 wells completed within this "semi-confined" aquifer and 25 wells in the overlying residuum. Calcium and bicarbonate made up - 90% of the ionic load of ground water and the bicarbonate/calcium ion ratio closely approximated 2:1, indicating that the dissolution of calcite was the dominant reaction controlling major ion chemistry in the UFA. Ground water is saturated with respect to calcite within the lower portion of the residuum and does not evolve from undersaturated to saturated conditions along down gradient flow paths within the UFA itself. The calcite saturation indices for 87% of the UFA wells were between -0.25 and +0.25 SI_{cal} units. This stands in contrast to those locations where the UFA is confined and ground water evolves from an undersaturated condition towards a state of equilibrium with calcite. Calcium ion concentrations vary from 0.7 to 2.0 mmol/L indicative of a variable degree of calcite dissolution. The Ca^{+2}- PCO_2 relationship closely conformed to the theoretical equilibrium between CO_2, calcite, and dilute water which dictates that calcite dissolution varies as the cube root of PCO_2.

INTRODUCTION

The objective of this study was to determine the effects of semi-confining conditions upon the evolution of the aqueous carbonate system (H_2O-CO_2-$CaCO_3$) of ground water within the Upper Floridan aquifer (UFA). The Dougherty Plain comprises a significant portion of southwestern Georgia and therefore provides an opportune location for this study. Previous geochemical investigations have concluded that the presence or absence of a regional confining unit has a very important effect upon the evolution of ground-water chemistry within the UFA and elsewhere (Back and Hanshaw, 1970; Plummer, 1977; Wicks and Herman, 1994). Relatively few studies, however, have focused upon changes in ground-water chemistry within carbonate aquifer systems that are "semi-confined" (Katz and others, 1995) such as the UFA in this study area.

STUDY AREA

The Dougherty Plain (see Figure 1) in southwestern Georgia is an extensive, nearly-flat, karst plain (Hayes and others, 1983) in close proximity to the updip margin of the Floridan or Principal Artesian aquifer (Miller, 1986). Approximately 1.5 million cubic meters of ground water is extracted daily from the UFA for soybean, cotton, and peanut crops grown in the 12-county study area. Additional ground water is used by the City of Albany for municipal purposes (Fanning, 2003). The UFA in this region is comprised of the Late Eocene aged chalky white to pink, fossiliferous Ocala Limestone that ranges in thickness from -0-110 meters and dips slightly to the southeast. Regional transmissivity values range from -280 to 46,000 m^2/day and the UFA yields as much as 7.5 cubic

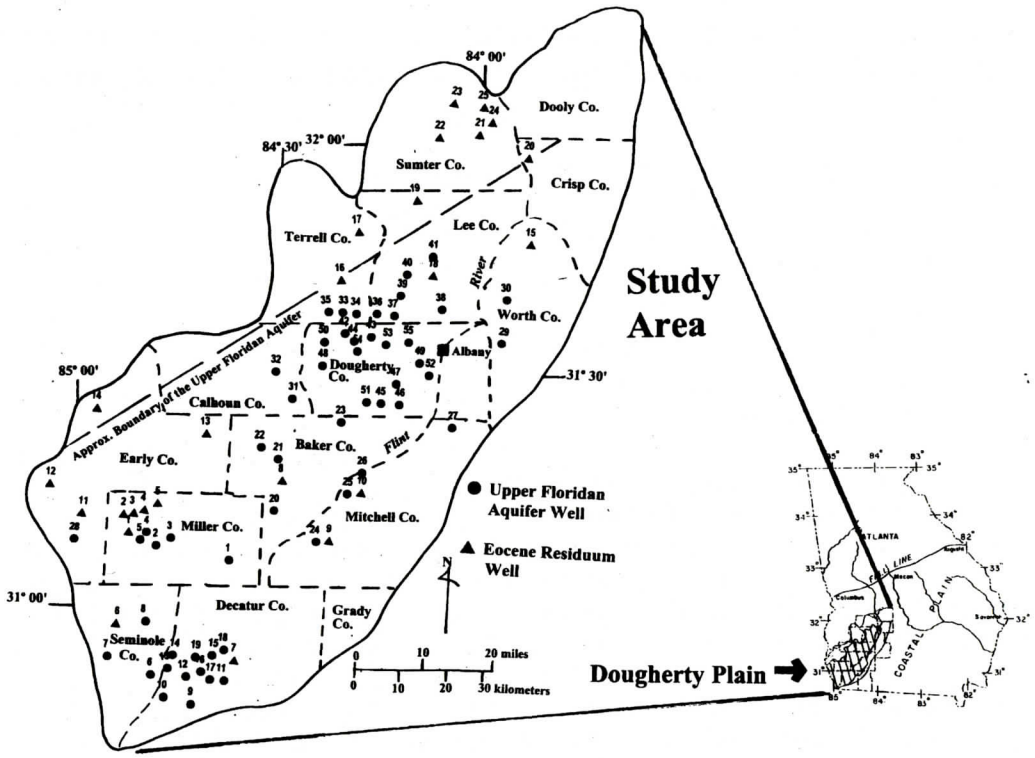

Figure 1. Map of the Dougherty Plain study area showing sample locations.

meters per minute (~2,000 gpm) at some localities (Hayes and others, 1983; Warner, 1997). The Ocala Limestone is exposed along the Flint River, which along with its tributaries represents the regional surface water drainage feature and principal ground-water sink. Numerous shallow circular depressions (filled in ancient sinkholes) are dominant geomorphologic features of the Dougherty Plain (Hicks and others, 1987).

The regional ground-water flow gradient is towards the south and southeast; however, it is likely that this system as most other systems in humid regions is dominated by "local flow cells" (Back and others, 1993). Clark and others (1997) concluded on the basis of isotopic and noble gas data that there is only a limited degree of mixing between local UFA recharge and deeper ground water. Trace amounts of pesticide, insecticides, and chlorinated solvents are present in selected wells completed near Albany in Dougherty County indicating that a component of modern water is present within the UFA (Hayes and others 1983; Hicks and others, 1987; Chapman, 1993). Hayes and others (1983) concluded that ground-water flow within the UFA in this study area is both *diffusive* (flow through pores) and *channeled* (flow through fractures and solution conduits).

For purposes of this study, the distinctive feature of the UFA in this study area is the absence of a regional confining unit (i.e. clay beds of the Miocene-aged Hawthorn Formation). The aquifer is covered locally by a red sandy clay residuum which is typically 12-20 meters thick that has been designated as a "semi-confining layer" (Hicks and others, 1981; Hayes and others, 1983). Locally the residuum is as great as ~40 meters thick and its clay content ranges between 10-70% (Watson, 1981). Most, if not all, of the residuum is derived from the Ocala Limestone (Plate 8; Miller, 1986) and some residuum is present in the northern portion of the Dougherty Plain above the updip limit of the Floridan aquifer (Figure 1). The Ocala Limestone is underlain by the Lisbon Formation that consists of

Table 1. Summary of Hydrochemical Data

	Temp °C	Spec. Cond[1]	TDS[2]	pH	Ca	Mg	Na	K	SO_4	Cl	HCO_3	NO_3	Silica	logPCO_2[3]	Calcite Saturation Index[4]
Eocene Residuum (n=25)															
Minimum	16.8	17	24	5.0	0.1	0.02	<0.1	<0.1	<0.1	1.8	4	<0.05	3	-3.11	-6.29
Maximum	24.4	278	240	7.8	78	1.6	8.4	1.9	16	6.1	161	3.7	43	-0.98	0.06
Mean	20.8	118	105	6.5	24	0.6	3.0	0.4	2.5	3.4	64	1.2	10.0	-2.02	-2.22
Standard Deviation	1.6	82	72	1.0	21	0.4	1.3	0.5	3.5	1.3	46	1.1	7.9	0.057	2.03
Upper Floridan Aquifer (n = 55)															
Minimum	17.5	178	142	6.8	33	0.1	1.3	<0.1	<0.2	<0.2	90	<0.1	5.2	-3.18	-0.62
Maximum	22.6	592	515	8.1	110	11	22	2.6	33	20	312	11	24	-1.77	0.48
Mean	20.6	262	219	7.5	48	1.8	2.5	0.4	1.9	4.1	149	1.8	8.5	-2.38	-0.11
Standard Deviation	1.0	45	39	0.3	10	2.6	2.8	0.3	1.9	1.8	28	1.9	4.2	0.29	0.19

[1]μS/cm; [2]All concentrations in mg/L; [3]computed values; [4]WATEQF computed values

a hard, well-cemented sandy-clayey-limestone comprising the base of the Principal Artesian aquifer in the study area (Hayes and others, 1983).

METHODS

The hydrochemical data were derived from the United States Geological Survey (USGS) database (US Geological Survey, 2003). Most of the water samples in this database were collected from production wells and were analyzed using methods employed by the USGS. In all cases alkalinity and pH were determined in the field. A final set of 80 well samples was derived based upon the completeness and accuracy of their analysis, well location (Figure 1), and sample collection date. Fifty-five of the samples were representative of ground water within the UFA and 25 of the samples were from the overlying Eocene residuum (following the terminology used by the USGS). Some of the residuum wells were located in updip locations (Figure 1) where the Ocala Limestone is either not present or too thin to be designated as the UFA. Eighty percent of the analyses were derived from the period between 1992-2000 and these were supplemented by additional data from the period between 1981-1983.

The potentiometric surface of the UFA within the Dougherty Plain region varied only slightly between 1985 and 1999 (i.e. typically less than 2.5 meters of difference in ~40-80 meters of total hydraulic head) which is consistent with earlier reports (Hicks and others, 1987). Therefore, since it can be assumed that the ground-water flow regime has remained nearly temporally invariant, the utilization of ground-water data from these different periods should not introduce significant biases. Major ion (Na, Ca, Mg, K, Cl, SO_4, HCO_3, SiO_{2aq}, temperature, and pH) data were input into the speciation program WATEQF (Plummer and others, 1976) used to calculate total dissolved solids (TDS) concentrations, activity coefficients, ionic activities, mineral-water saturation indices, partial pressure of carbon dioxide activity (PCO_2) and percentage error. The average analytical error for the total sample set (n=80) was 2.0% and the maximum permissible error was 6.0%. The complete set of chemical data is not published herein but is available upon request.

RESULTS AND DISCUSSION

Chemical Characteristics

Mean TDS concentrations within the UFA and the Eocene residuum are 219 ± 39 (±1σ)

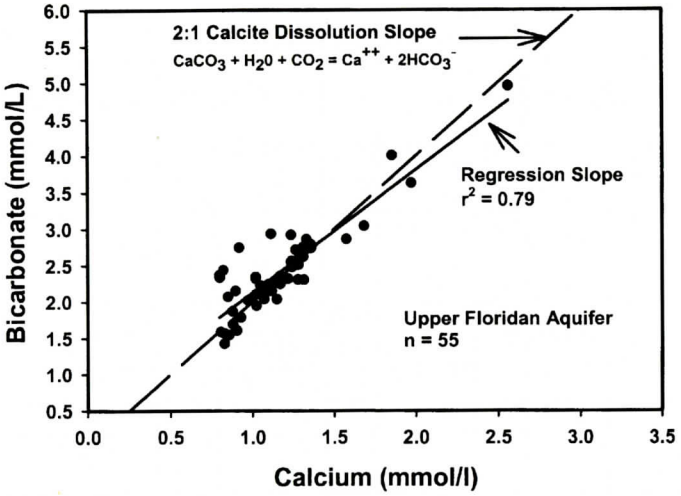

Figure 2. Trend analysis for calcium and bicarbonate ion molar concentrations within the UFA.

and 105 ± 72 mg/L respectively (Table 1) - well within drinking water limits. The mean pH for UFA ground water (7.5) is one unit greater than that of ground water within the residuum. Calcium and bicarbonate are by far the dominant ions and comprise on average 88.0 ±7.8% and 91.4% ± 4.4% of the percentage equivalence of cations and anions respectively. Concentrations of the other major ions are very low (typically less than 5 mg/L within the UFA) and mean sodium, silica, and sulfate concentrations are slightly higher within the residuum than in the UFA (Table 1).

The chemical composition of UFA ground water strongly suggests that the dissolution of calcite ($CaCO_3$) is the governing geochemical process, as would be expected in a limestone aquifer. Calcium carbonate congruently dissolves in carbonic acid solution to produce an ideal 2:1 HCO_3^-/Ca^{+2} molar ratio:

$$CaCO_3 + H_2O + CO_2 \text{ ----> } Ca^{+2} + 2\,HCO_3^- \quad [1]$$

The average molar ratio of the 55 UFA analyses was 2.09 ± 0.31 and this near-2:1 HCO_3^-/Ca^{+2} ratio applies throughout the range of ground water compositions (Figure 2). Greater deviation from this ideal slope and higher ionic loads would be expected if silicate dissolution, ion exchange, or any geochemical processes in addition to the dissolution of calcite were occurring to a significant extent within the UFA.

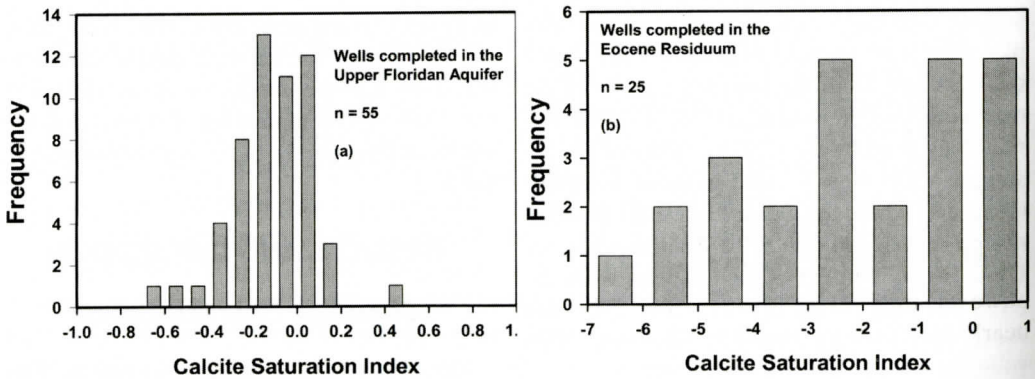

Figure 3. Histograms showing the distribution of calcite saturation indices (SI_{cal}) for (a) the Upper Floridan aquifer and (b) the residuum.

Calcite Saturation

A key parameter for assessing the chemical evolution of ground water in carbonate aquifers is the calcite saturation index (SI_{cal}), defined as follows:

$$SI_{cal} = \log_{10} \frac{(Ca^{+2})(CO_3^{-2})}{K_{eq}} \qquad [2]$$

where (Ca^{+2}) and (CO_3^{-2}) are the WATEQF-calculated activities of calcium and carbonate ion and K_{eq} is the equilibrium constant for the congruent dissolution of calcite at the ambient temperature of ground water. SI values of zero indicate the ground water is in equilibrium with calcite while negative and positive values respectively indicate undersaturated and oversaturated conditions. Fifteen of the 25 residuum ground-water samples were unequivocally undersaturated with respect to calcite ($SI_{cal} < -1.0$) [Figure 3]. Conversely, 87% of SI_{cal} values for the UFA were between ±0.25, which strongly implies equilibrium conditions between calcite and ground water. Only three of the UFA analyses were characterized by SI_{cal} values less than -0.5 (Figure 3). These results somewhat contradict an earlier study (Sprinkle, 1989) in which ground water was reported to be undersaturated with respect to calcite below the calcareous residuum.

Spatial Trends

A detailed analysis of the saturation state of ground water with respect to calcite in the Eocene residuum reveals an interesting trend. Shallow ground water (i.e. at total well depths of less than 16 meters which is the average thickness of the residuum) is in most cases greatly undersaturated with respect to calcite ($-6.3 < SI_{cal} < -0.5$; Figure 4). At greater depths (16-30 meters), some ground water remains undersaturated with respect to calcite; however, the SI_{cal} for most of the wells was nearly zero (Figure 4) indicating that ground water equilibrates with calcite (present within the residuum) above the top of the UFA.

Major spatial variation with respect to SI_{cal}

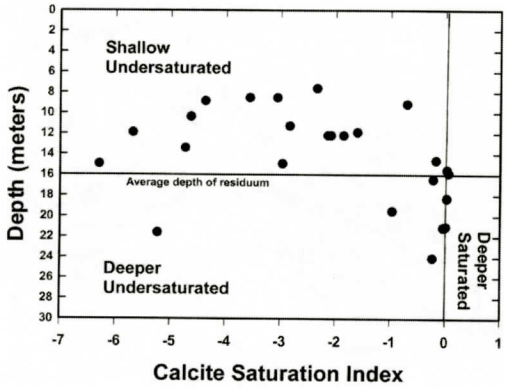

Figure 4. Calcite saturation indices (SI_{cal}) for ground water in the residuum overlying the UFA. Note that most of the deeper ground water in the residuum is saturated with respect to calcite while most of the shallow ground water is undersaturated. The horizontal line represents the average depth of the residuum and the vertical line represents the calcite-saturated condition.

values in the UFA itself might not be expected if ground-water recharge becomes saturated with respect to calcite in the semi-confining residuum. To test this hypothesis, saturation indices, bicarbonate alkalinity values, and calculated PCO_2 values were compared in 11 "upgradient" and 8 "downgradient" wells. The upgradient wells were located northwest of Albany near the updip limit of the Floridan aquifer and the downgradient wells were located -25 kilometers south along a probable ground-water flow path (Figure 5). There are -18 meters of difference with respect to potentiometric levels between the two sets of wells. The mean SI_{cal} for the upgradient and downgradient wells is -0.14 and -0.09 respectively. T-tests confirm that there is no significant difference (α=0.05) between the saturation indices for the two sets of wells. Likewise, the results of similar t-tests indicate there is no significant difference (α=0.05) between mean bicarbonate concentration values ($HCO_{3\ mean\ upgradient}$ = 2.56 mmol; $HCO_{3\ mean\ downgradient}$ = 2.37 mmol/L) nor log PCO_2 values ($\log PCO_{2\ mean\ upgradient}$ = -2.38 atm; $\log PCO_{2\ mean\ downgradient}$ = -2.42 atm) for the two sets of wells. Unlike at some other UFA locations, ground water below the Dougherty

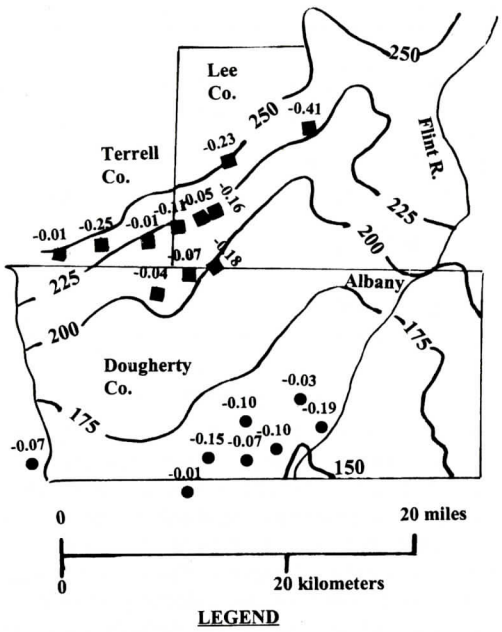

Figure 5. Calcite saturation indices for ground water in selected Upper Floridan aquifer wells. The SI_{cal} for the upgradient wells (indicated by squares) are very similar to the SI_{cal} values wells for the downgradient wells.

Plain does not appear to undergo a significant chemical evolution as it flows downgradient from its recharge area (see discussion below).

Ca-PCO_2 Relationship and Its Effect Upon the Geochemical Evolution of Ground Water

Calcium ion concentrations vary between 33-110 mg/L within UFA ground water below the Dougherty Plain. This is indicative of variable degrees of calcite dissolution in that this reaction is the only plausible major source of calcium. At first this might appear to be enigmatic in that ground water is either saturated or very closely saturated with respect to calcite throughout the study area. However, a variable degree of calcite dissolution can occur as a function of the partial pressure of carbon dioxide (PCO_2) in ground water that is in equilibrium with calcite.

The relationship between Ca^{+2} and PCO_2 in equilibrium with calcite at a given water temperature is as follows (after Drever, 1997):

$$[Ca^{+2}] = K^* \times PCO_2^{1/3} \times 1{,}000 \qquad [3]$$

where:

$$K^* = \{K_1 \times KCO_2 \times K_{cal} \times (4K_2)^{-1}\}^{1/3} \qquad [4]$$

and $[Ca^{+2}]$ = calcium ion concentration in mmol/l, PCO_2 = partial pressure of CO_2 in water (atm); K_1 = first dissociation constant for carbonic acid, K_2 = second dissociation constant for the bicarbonate ion, KCO_2 = equilibrium constant for the partitioning of carbon dioxide in water, and K_{cal} = the equilibrium constant for calcite dissolution. The pK values used for K_1, K_2, K_{CO2}, and K_{cal} at 20°C are 6.38, 10.38, 1.41, and 8.45 respectively (from Drever, 1997). Equations 3 and 4 are based upon the assumptions that the concentrations of the other ions are sufficiently dilute such that the charge balance can be satisfied solely by Ca^{+2} and HCO_3^- and that the activity coefficients for these two ions are equal to 1.0 (an assumption that closely conforms to the WATEQF output).

Equation 3 dictates that calcium ion concentration should increase only to the extent of the cube root of PCO_2 if ground water is in equilibrium with calcite. Calculated log PCO_2 values vary within UFA ground water by approximately two orders of magnitude (from -3.17 to -1.77; Table 1). The cause of this variation is not explicitly known; however, it might be the result of variable quantities of metabolically active organic matter in recharge areas. A plot of calcium ion concentrations versus PCO_2 reveals that approximately 90% of the 55 analyses closely conform to the ground water-calcite equilibrium condition that is represented by the solid parabolic curve on Figure 6. Furthermore, the data points are close to the theoretical pre-

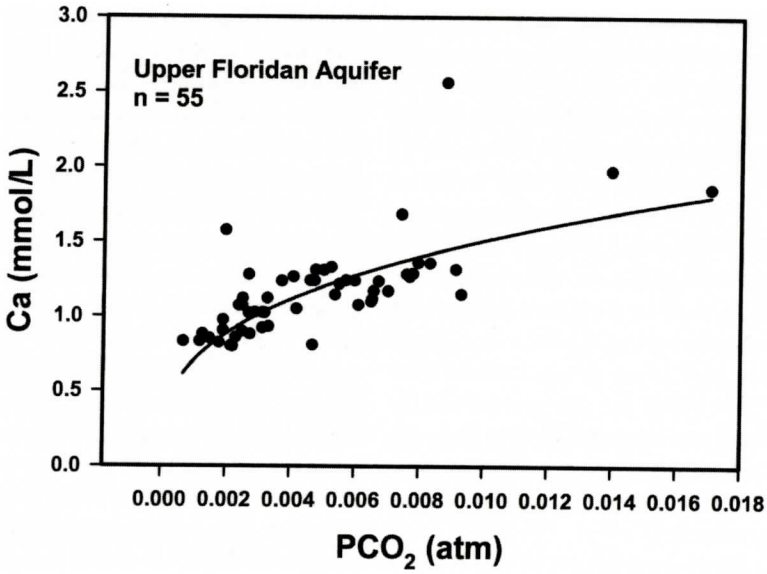

Figure 6. Distribution of calcium and computed PCO_2 values plotted with respect to the theoretical equilibrium curve (solid line) between calcite, PCO_2, and ground water (see text for explanation).

diction over the range of PCO_2 values calculated for ground water in the UFA. The few outliers can be viewed as exceptions to the general condition of equilibrium. In short, the dominant process controlling the chemical composition of the UFA below the Dougherty Plain is the extent to which aqueous carbon dioxide dissolves calcite to equilibrium with ground water. The degree to which the ionic load of ground water can increase as a result of calcite dissolution is inherently limited by both the diffusion of carbon dioxide into ground water and the cube root relationship governing calcite dissolution (Equation 3).

The Effects of Aquifer Confinement

The degree to which an aquifer is confined is a major hydrogeologic variable in controlling aquifer chemistry in Coastal Plain aquifers. This is the case because unconfined aquifers ideally behave as "open systems" allowing for the steady influx of dilute ground water (undersaturated with respect to calcite), carbon dioxide, and other components (Wicks and Herman 1994; Back and others, 1993). Specifically, Wicks and Herman (1994) noted that where the UFA in western-central Florida is leaky or unconfined, calcite dissolution occurs along most of the ground-water flow path due to the uninhibited influx of undersaturated recharge waters and the ingassing of CO_2. Plummer (1977) concluded from a modeling study that ground water retains supersaturated conditions with respect to Mg-calcite in the portion of the UFA in central Florida that remains closed to CO_2 (i.e. where the Hawthorn Formation provides a regional confining unit above the Ocala Limestone). Back and Hanshaw (1970) observed that ground water within the confined portion of the UFA in north central Florida evolves from calcite-undersaturation in recharge areas to calcite-supersaturation downgradient along flow paths. In contrast, ground water within age-equivalent rocks of the Yucatan Peninsula does *not* evolve in that regional flow paths do not exist. Ground water within this unconfined aquifer flows from one karst feature to another and is in most cases supersaturated with respect to calcite.

The UFA below the Dougherty Plain represents an "intermediate" condition between a totally confined and unconfined aquifer in that it is only locally confined by its own residuum.

The UFA is to an extent "open" to the ingassing of CO_2 in that calculated partial pressures of CO_2 are typically one order of magnitude or greater than atmospheric ($logPCO_2 = -3.5$). The range of calculated pressures ($10^{-3.18}$ to $10^{-1.77}$ atmospheres) is similar to other UFA locations (e.g. $10^{-2.9}$ to $10^{-1.7}$ atmospheres in western central Florida; Wicks and Herman, 1994). The key difference with respect to the evolution of the carbonate system in these two locations is that there is no compelling evidence that calcite dissolution occurs along ground-water flow paths in the UFA below the Dougherty Plain. In contrast, Wicks and Herman (1994) have inferred that calcite dissolution occurs in West Central Florida where the UFA system is either leaky or unconfined.

The most likely explanation is that there is abundant calcite within the "semi-confining" residuum in the Dougherty Plain region as opposed to other Coastal Plain locations where the aquifer is either totally unconfined or overlain by sand deposits. Recall that ground water within the upper residuum (<16 meters) is well undersaturated with respect to calcite ($SI_{cal} < -2.0$) while in the lower residuum ground water approaches calcite saturation (Figure 4). Apparently, the clay content of the residuum is sufficiently high as to allow enough contact time for ground-water recharge to equilibrate with calcite. The ingassing of CO_2 to the aquifer likely occurs throughout the Dougherty Plain to some extent. This results in variable degrees of calcite dissolution with related effects upon calcium concentrations and alkalinity. However, in the semi-confined aquifer there are no systematic downgradient changes with respect to SI_{cal} values as is often the case in confined aquifers.

SUMMARY AND CONCLUSIONS

The major ion chemistry of ground water within the UFA below the karstic Dougherty Plain in southwestern Georgia is controlled almost totally by the dissolution of calcite. This is evidenced by the high percentage (~90%) of calcium and bicarbonate and the nearly ideal 2:1 HCO_3^-/Ca^{+2} ratio in most ground water samples. Equilibrium between ground water and calcite appears to occur within the lower portion of the Eocene residuum that overlies the aquifer as a "semi-confining" unit. Additional calcite dissolution occurs locally below the residuum as the result of CO_2 ingassing. The UFA is more or less open to the ingassing of CO_2 and the extent to which calcite dissolves is ultimately governed by the partial pressure of CO_2 in ground water. Calcium ion activities and computed PCO2 activities closely conform to the cube-root equilibrium relationship between calcite and carbon dioxide in dilute ground water. The calcareous and argillaceous residuum overlying the UFA certainly allows for recharge to occur throughout much of the Dougherty Plain. However, this recharge is typically chemically evolved to the point where ground water in the UFA is saturated with respect to calcite and then does not systematically evolve further along downgradient flow paths. This is in contrast to those locations where the UFA is confined and ground water typically evolves from an undersaturated to a calcite-saturated state.

ACKNOWLEDGEMENTS

I would like to thank *Southeastern Geology* reviewers Jack Eggleston and Terri Woods for their many constructive comments that helped to significantly improve the quality of this paper.

REFERENCES

Back, W.M. and Hanshaw, B.B., 1970, Comparison of the chemical hydrogeology of the carbonate peninsulas of Florida and Yucatan: Journal of Hydrology, v.10, p. 330-368.

Back, W.M., Baedecker, M.J., Wood, W.W., 1993, Scales in chemical hydrogeology: a historical perspective: *in* Alley, W.M. (editor) Regional Ground-Water Quality. Van Nostrand Reinhold, New York, p. 111-129.

Chapman, M.J., 1993, Ground-water quality of the Upper Floridan aquifer near an abandoned manufactured gas plant in Albany, Georgia: USGS Water Resources Investigation Report, 93-4038, 19 p.

Clark, J.F., Stute, M., Schlosser, P., and Drenkard S., 1997, A tracer study of the Floridan aquifer in southeastern Georgia: implications for groundwater flow and paleoclimate: Water Resources Research, v.33, p. 281-289.

Drever, J.I., 1997, The Geochemistry of Natural Waters 3rd

ed.: Prentice Hall, Upper Saddle River, New Jersey, 436 p.

Fanning, J.L., 2003, Water use in Georgia by county for 2000 and water-use trends for 1980-2000: Georgia Geologic Survey Information Circular 106, 176 p.

Hayes, L.R., Maslia, M.L.,Weeks, W.C., 1983, Hydrology and model evaluation of the principal artesian aquifer, Dougherty Plain, southwest Georgia: Georgia Geologic Survey Bulletin 97, 93 p.

Hicks, D.W., Gill, H.E., Longsworth, S.A., 1987, Hydrogeology, chemical quality, and availability of ground water resources in the Upper Floridan aquifer, Albany area, Georgia: U.S. Geological Survey Water Resources Investigation Report 87-4145, 52 p.

Katz, B.G., Plummer, L.N., Busenberg, E., Revesz, K.M., Jones, B.F., Lee, T.M., 1995, Chemical evolution of groundwater near a sinkhole lake, northern Florida 2. Chemical patterns, mass transfer modeling, and rates of mass transfer reactions: Water Resources Research, v.31, p. 1565-1584.

Miller, J.A., 1986, Hydrogeological framework of the Floridan aquifer system in Florida and in parts of Georgia, Alabama, and South Carolina: U.S. Geological Survey Professional Paper 1403-B, 91 p.

Plummer, L.N., Jones, B.F., Truesdell, A.H., 1976, WATEQF: a FORTRAN IV version of WATEQ, a computer program for calculating equilibrium of natural waters - user's guide: U.S. Geological Survey Water Resources Investigation Report 76-13, 61 p.

Plummer, L.N., 1977, Defining reactions and mass transfer in part of the Floridan aquifer: Water Resources Research, v.36, p. 801-812

Sprinkle, C.L., 1989, Geochemistry of the Floridan aquifer system in Florida and parts of Georgia, South Carolina, and Alabama: U.S. Geological Survey Professional Paper 1403-I, 105 p.

U.S.Geological Survey, 2003, Water data for Georgia: http://waterdata.usgs.gov/ga/rwis/qwdata.

Warner, D., 1997, Hydrogeologic evaluation of the Upper Floridan aquifer in the southwestern Albany area, Georgia: U.S. Geological Survey Water Resources Investigation Report 97-4129, 27p.

Watson, T.W., 1981, Geohydrology of the Dougherty Plain and adjacent area, southwest Georgia: Georgia Geologic Survey Hydrological Atlas, 5 plates.

Wicks, C.M., Herman J.S., 1994, The effect of a confining unit on the geochemical evolution of ground water in the Upper Floridan aquifer: Journal of Hydrology, v.153, p. 139-155.